AN ABSTRACT OF THE THESIS OF

Aaron Wilmot for the degree of Master of Science in Radiation Health Physics presented on June 25, 2009.

Title: A Comparative Evaluation of the Health Risks from Minor Actinide Fission Products

Abstract approved:

Jack F. Higginbotham

Abstract text

In consideration of the potential use of minor actinides in nuclear fuel, the fission products of several minor actinides (^{237}Np, ^{241}Am, ^{242m}Am, ^{243}Cm, ^{244}Cm, ^{245}Cm, and ^{246}Cm) were evaluated and compared to the fission products of ^{235}U. Available data from the Evaluated Nuclear Data File and the Nuclear Database were used in conjunction with Environmental Protection Agency risk estimates and the Radiological Safety Analysis program to estimate several risks from the various fission products. Results show that some minor actinides produce fission products whose estimated risks are greater than the risks from fission products of ^{235}U in a number of cases.

A Comparative Evaluation of the Health Risks from Minor Actinide Fission Products

by

Aaron Wilmot

A THESIS

Submitted to

Oregon State University

In partial fulfillment of

the requirements for the

degree of

Master of Science

Presented June 25, 2009

Commencement June 2010

Master of Science thesis of Aaron Wilmot presented on June 25, 2009

Approved:

Major Professor, representing Radiation Health Physics

Head of the Nuclear Engineering and Radiation Health Physics Department

---

Dean of the Graduate School

I understand that my thesis will become part of the permanent collection of Oregon State University libraries. My signature below authorizes release of my thesis to any reader upon request.

Aaron Wilmot, Author

ACKNOWLEDGEMENTS

The work presented here is a small step beyond the massive strides that have already been taken in the discipline. There are many individuals who have affected this work, either directly or indirectly, as it has progressed. This page is an attempt to thank all of those who have shaped this project– it could not have been completed without the help of a long list of people.

Lacking the guidance, help, and support of my advisor, Dr. Jack Higginbotham, this work would not have even been initiated. I am fortunate to have been able to perform this work for such a knowledgeable, respected, and kind individual.

The members of my committee have also gone above and beyond (including staying after normal working hours) to aid me in this endeavor. Without Drs. Higley, Narayanan, and Woods, this document could not have been completed. I thank them for their efforts, feedback, and support.

I would also like to thank Dr. Bradley Schrader of the Idaho National Laboratory for the use of the Radiological Safety Analysis Code, which was very helpful in the evaluation.

There is another lengthy collection of individuals who have provided encouragement and guidance, be it either technical or professional in nature, leading me down a path that has culminated in this work. In this regard, I would like to thank my family (both immediate and extended), Messrs. Gentile and Blair, and Mrs. Meigs-Alvarez.

TABLE OF CONTENTS

Page

LIST OF FIGURES

LIST OF TABLES

LIST OF APPENDICES

LIST OF APPENDIX FIGURES

LIST OF APPENDIX FIGURES (Continued)

Figure Page

LIST OF APPENDIX FIGURES (Continued)

LIST OF APPENDIX TABLES

DEDICATION

This work could not have been completed (or even initiated) without the support of my loving wife, Kara. For her, and for her constant encouragement, I will always be grateful.

A COMPARATIVE EVALUATION OF THE HEALTH RISKS FROM MINOR ACTINIDE FISSION PRODUCTS

Introduction

While writing this paper, the topic of energy generation is receiving an enormous amount of attention within the United States and across the globe. Politicians and leaders are shaping policies to address a growing need for more electricity. Researchers, scientists, and engineers are grappling with complex technical issues in an attempt to find a feasible, cost-effective means of solving the energy dilemma.

One of the topics being put forward within the United States involves recycling. However, the recycling addressed here does not involve household items such as paper or plastic, but significant quantities of used (or spent) nuclear fuel, SNF (Baetsl, 1997). The U.S. Department of Energy (DOE) and other research institutions have been developing nuclear reactor designs intended to take portions of this SNF and find practical ways to consume the useful portions of this material while producing electricity.

On other scientific frontiers, alternate means of propulsion are being examined to further space exploration (Gurion, 2001). Some of these plans for powering craft suitable for space exploration involve nuclear energy, and specifically, alternate forms of nuclear energy compared to the typical commercial nuclear power reactors or radioisotope thermal generators previously considered. A recent concept suggests using fissile material constructed from a minor actinide (MA) produced in nuclear reactors; namely ^{242m}Am.

These fields of study, along with the discipline of health physics, are bound together with a common theme – the health risks from fission products (FPs) of MAs. Whether licensing a new reactor design (or a new reactor fuel loading), or operating a nuclear plant with failed Mixed Oxide (MOX) fuel, the FP of MAs could be a significant technical and health concern.

This paper is intended to address the issue: the health risks and effects of the FP of the MAs. The initiating fission event, within this paper, is assumed to arise from an incident neutron in the thermal energy range.

Literature Review

Several nuclear reactor designs have been analyzed and presented which rely on, or allow for the use of MOX fuel. A majority of the MOX fuel fabricated and addressed to date consists of plutonium as the fissile nuclide (World Nuclear Association, 2009).

Concepts for other designs have included fuel elements or arrays containing quantities of a MA nuclide – such as ^{241}Am, ^{242m}Am, ^{237}Np, ^{243}Cm, ^{244}Cm, ^{245}Cm, or ^{246}Cm (Westlén, 2007). Other designs have noted the importance of these nuclides in helping to decrease the proliferation risk from spent nuclear fuel (Yoga, 2005), and have called for increased quantities of these materials as additives in the fuel. All of these nuclides are produced in typical light water nuclear reactors using ^{235}U as the primary fissile nuclide. Their production results from either a double (or triple, or greater) neutron capture in ^{235}U, or another nuclear reaction in an impurity in the nuclear fuel. The end result of this capture process is a nuclide that was considered a waste until recently (Sahin, 1984).

A significant amount of research effort has been applied to nuclear physics aspects of MA s and MA fission (Bergelson, 2004). However, bodies of work on the health physics aspects of these nuclides are not as readily available. Some previous works have addressed related issues, such as external dose rates (Sasahara, 2004), but the internal exposure implications of these FP have not been extensively documented.

Materials and Methods

To help establish the risks expected from MA FP, a methodical approach using available data will be used. This section outlines the resources, tools, and procedures that were used in an attempt to comparatively analyze the FP of the nuclides identified above. While recognizing that not all potential exposure pathways or scenarios could be considered, some of the most frequent or historically significant exposure pathways were analyzed as part of this work. The intended result is a reasonable, credible comparison of the risks result from these FP. The aim of the work is to provide information that would be valuable when developing emergency procedures, nuclear material controls, new nuclear reactor designs or fuel loadings, and health physics programs.

First, all data will be normalized to a single fission resulting from a neutron in the thermal energy range. This allows a comparison of results from various fissile nuclides on a common basis. Practically, the data or results of this work can be applied to any situation using a scaling factor based upon the number of fissions that have occurred.

Additionally, nuclides arising from sources other than fission will be excluded from this evaluation. For example, many activation nuclides, transmuted actinides, or unused fuel nuclides are often included in radiological assessments involving FP. Many of these nuclides have significant effects on the outcome of any dose estimates (Ivanova, 1995). The composition and specifics of these nuclides vary greatly with the environment and situation in which they are produced. By excluding these constituents, the results of this work may be more applicable to any situation involving FP, allowing other nuclides to be added and scaled as needed.

To properly address the health risks of the MA FP, first the FP themselves need to be identified or defined. With a technical definition of the FP of each fissile nuclide selected in this study (^{235}U, ^{237}Np, ^{241}Am, ^{242m}Am, ^{243}Cm, ^{244}Cm, ^{245}Cm, and ^{246}Cm)[1], by radionuclide yield,

[1] Note that ^{235}U is selected to serve as a reference, since a majority of fission product analyses have focused on the fission products from the thermal fission of ^{235}U.

the work of analyzing the health risks from these FP can begin. The parameters of interest for this evaluation are:

- Activity of Selected Radionuclides
- Total Radioactivity
- Photon Exposure Rate
- Emitted Energies
- Inhalation Risk
- Ingestion Risk
- Submersion Risk
- Estimated Risks following a Fission Product Release

The sections below describe the processes used to arrive at estimates and comparisons of each of the parameters identified above.

Obtaining Fission Yield Data

Fission yield data for ^{235}U and ^{239}Pu is widely available (Knolls, 2002), while fission yields for the MAs mentioned above are not as well publicized. This does not mean that the subject hasn't received attention from researchers and scientists, however. For example, several recent works have focused on the topic (Shinohara, 1999).

Previous works have also evaluated the fission yields from the MAs. One of the most recent publications of evaluated nuclear data on the topic of fission yields was produced by Los Alamos National Laboratory, LANL (England, 1995). This data was used, in part, to populate the Evaluated Nuclear Data File (ENDF) maintained by Brookhaven National Laboratory (BNL). ENDF contains a variety of nuclear data; from nuclear cross sections, to fission yields, to decay data. The fission yield data from ENDF (Chadwick, 2006) was selected for use in this work.

To obtain usable data from the ENDF information, a Visual Basic application was written to convert from the ENDF VI formatted output files to columnar data presented in MicroSoft Excel. The end result was a radionuclide distribution, containing fission yields for each radionuclide along with fission yield uncertainties. All of this information was saved in spreadsheets and databases to enable a more efficient data manipulation.

Obtaining Radionuclide Decay and Emissions Data

The next step in obtaining risk estimates required a conversion of the available fission yield data. The data obtained from the ENDF file above was a distribution of the number of atoms of each fission product following a split of the initial fissile nuclide. This was verified by summing the fission yields, and noting that the total was approximately two. However, as opposed to the number of atoms, most risk estimates require a measure of the radioactivity of a radionuclide, and not the number of atoms of a given radionuclide. This conversion is straightforward, using the equation below for any nuclide, *i*:

$$A_i = \lambda_i N_i$$

The decay constant, λ, for each radionuclide must be found and multiplied with the number of atoms obtained from the ENDF files above.

In this case, again the ENDF file was considered as a primary reference. The ENDF library did not present data in a form that was as easy to manipulate as recent electronic publication of existing International Commission of Radiological Protection (ICRP) data (ICRP, 1983) by Stabin (2002). However, the electronic data from ICRP 38 was found to be less complete than the online emissions data maintained by BNL as part of the NNDC. As a result, the NuDat electronic resource was selected as the source for decay constants used in this work (National Nuclear Data Center). The Nuclear Data (NuDat) database is similar to ENDF in that this resource contains a variety of nuclear data and is maintained by BNL as part of the NNDC. However, the NuDat database allows users to request output in a format that is much easier to convert to spreadsheet or database files without the use of a Visual Basic macro or other computer application.

For this reason, the NuDat data for nuclides whose atomic number lies between 65 and 180 were requested and summarized in a database format. The NuDat data consists not only of decay constants, but also each radionuclide emission, including emission type, energy, frequency, and other relevant information.

Using Decay Data to Convert Fission Yields to Radioactivity Yields

As mentioned above, the fission yields obtained from ENDF can be converted to radioactivity using an appropriate decay constant. Linked tables in an Access database were used to store the fission product yields along with the NuDat data, and relationships and cross-references were established to multiply each radionuclide by the corresponding decay constant.

Selecting Specific Radionuclides of Interest

To identify nuclides with specific health physics connotations in most fission product distributions, existing lists of relevant nuclides and historical data were reviewed.

The Department of Energy has published several documents that can be very useful when evaluating relative risks from FP. A primary source is the Federal Radiological Monitoring and Assessment center (FRMAC) manual (DOE, 2007). This manual is intended to serve as a significant source of information when planning for, or responding to a radiological or nuclear incident.

The FRMAC manual evaluates several credible scenarios involving radiological or nuclear events. These scenarios include a nuclear power reactor accident followed by a release of FP to the environment, an RDD event, and a nuclear weapon detonation. The evaluation of a nuclear power accident includes a relevant list of fission product radionuclides that are expected to be relevant following the accident. The nuclides were selected on the basis of projected health risks through one of several exposure pathways. Other assessments of FP (Renaud, 2004) were also reviewed to identify nuclides that might not have been identified in the FRMAC manual.

The FRMAC manual also contains radiologically pertinent information regarding other exposure scenarios. However, for these exposure scenarios, FP are not indicated as a primary source of risk. For example, for RDD events or nuclear weapons detonations, the FRMAC manual estimates that the majority of the dose will be from transuranics or from probable RDD source nuclides, such as ^{60}Co.

The list of fission product nuclides that present significant health risks following a light water reactor accident will be used to compare the FP from the nuclides selected in this study. The list of fission product nuclides, taken from in the FRMAC manual (DOE, 2007), is shown below.

Table 1. FRMAC Fission Product Nuclides of Importance. The fission product radionuclides identified by the FRMAC manual are shown below.

Ba-140	Cs-137	I-135	Sb-129	Te-132
Ce-141	I-131	La-140	Sr-89	Xe-135
Ce-144	I-132	Nb-95	Sr-90	Y-90
Cs-134	I-133	Ru-103	Te-129m1	Y-91
Cs-136	I-134	Ru-106	Te-131m1	Zr-95

The fission yields of these radionuclides (immediately following fission) will be identified and compared.

Radiological Decay

To help compare risks in a more practical sense, an evaluation of decayed fission product distributions was included in this body of work. Practically, the engineer or health physicist would not expect to encounter a large number of situations where fresh FP are the radiological insult (that is, situations where the time between the initiating fission events and exposure is approximately 0 seconds). Realistically, if an exposure situation were to take place involving MA FP, there would be a finite time interval between the initiating fission event and the uptake or exposure. This time interval could include, as examples, transport from a failed fuel rod to a spent fuel pool to the airborne environment above the pool to the

breathing zone of a worker, or the time for fallout from a nuclear weapon to deposit in an area some distance away.

The time periods of 0, 1, 3, 10, 30, 100, 300, 1000, and 3000 seconds were selected for evaluation. This encompasses a span of 50 minutes; a time period in which a number of credible short-lived exposure scenarios are possible. Exposure scenarios further in time from the initiating fission events have also been documented (Beck, 1983 and Carbol, 2003). However, these scenarios were not analyzed as part of this work. Instead, other sections of this work address nuclides that have been noted to influence risks in these scenarios where the intake is significantly separated from the initiating fission event in time.

After a short time span, there are many factors and uncertainties that can significantly affect the risk posed from FP, including deposition, weather, solubility considerations, and environmental factors influencing uptake and distribution in biota. Evaluations of the risks from FP at longer time intervals are complex tasks that may eventually be addressed, but have not been analyzed in this paper.

To analyze the fission product distributions at the points in time selected above after the initiating fission event, some simplifications and assumptions were made. With each fission product distribution containing approximately 500 or more nuclides, many of which decay into other radionculides present that are also in the distribution, the effort involved in manually applying the Bateman equations (Shultis, 1999) to each nuclide in each distribution constituted a Herculean effort. To simplify the task in order to establish estimates at the time steps specified above, the Radiological Safety Analysis Code (RSAC) radionuclide decay function was applied (Schrader, 2005). In order to use this function, however, many short lived radionuclides were excluded from the calculations. Further justification and background for this assumption is provided below. A list of the nuclides that were excluded is shown in Appendix F.

With the relevant time steps selected and the means of radionuclide decay established, the work to evaluate the fission product distributions as a function of time was straightforward. First, each radionuclide distribution was formatted for RSAC; this involved slight changes in notation, and the removal of all nuclides that were neglected. Then, RSAC

inputs were developed to examine the fission product distributions from each radionuclide. The input files for each fission product distribution also contained a decay instruction to examine the decay of the fission product mixtures after a variety of times. The results of these decays would be used for further comparison and evaluation. A further description of the RSAC model and inputs is included below.

Obtaining Photon Exposure Rate Estimates

The gamma exposure rates produced by FP could have a significant impact on radiation doses to the public, first responders, or nuclear power plant workers in some contexts. To examine the effects that the nuclide undergoing fission has on these exposure rates, a methodical evaluation of the specific gamma ray constant for each fission product distribution will be conducted.

This evaluation will rely on NuDat published photon energies and intensities (National Nuclear Data Center, 2009). By using these intensities and energies, along with published expressions for deriving specific gamma ray constants, a gamma ray constant for each nuclide can be derived.

Mathematically, the exposure rate constant from a point source for a given nuclide can be found based upon photon emissions using the following (Cember, 1996 and Shultis, 2000):

$$\dot{X} = \frac{5.263 \cdot 10^{-6} \cdot 1 \cdot 10^{-4}}{3.7 \cdot 10^{10}} \sum_{all\ i} y_i E_i \left(\frac{\mu_{en}}{\rho}\right)_i$$

Where, for $\dot{X}$ to be obtained in units of $\left| \frac{R}{Ci \cdot hr} \right|$ at one meter, the quantities of E_i and $\left(\frac{\mu_{en}}{\rho}\right)_i$ must be in units of MeV and cm^2/g, respectively.

As shown in this expression, the exposure rate relies heavily on the $\left(\frac{\mu_{en}}{\rho}\right)$ term, or the mass energy absorption coefficient. Appendix C describes the methods used to obtain attenuation coefficients for each photon emission listed in NuDat.

To further evaluate the exposure rate effects of FP, the estimated exposure rate for each fission product distribution will be calculated at each point in time identified above.

Obtaining Emitted Energies

The NuDat database includes a term labeled as “dose” for each radionuclide emission. This quantity is defined in the NuDat glossary as “The product of a radiation energy times the probability per disintegration, the resulting unit is MeV×Bq-s.” While this exact term may not have an explicit health physics context, the quantity can be useful in comparing the emissions from two different distributions of radionuclides.

By summing the NuDat “dose” term for each radionuclide, and then multiplying the radionuclide-specific dose by the activity produced in fission of each of the nuclides being evaluated, an estimate of the energy emitted by each fission product radionuclide distribution can be established.

This evaluation of the energy emitted by each fission product distribution can be conducted as a function of time, as well, by evaluating the radionuclide distributions at each point in time separately. The results can provide a means of comparing the total amount of energy emitted by the FP as they decay. This comparison could serve as an indication of the possibility for biological damage (risk) if the FP were inhaled or ingested. However, an important consideration absent from this quantity is any relative radiation weighting factor that could be used to adjust for biological impact, particularly for ionizing radiations with high Linear Energy Transfer, such as alpha particles.

Obtaining Risk Estimates

To further compare and estimate the relative risks of various FP, published risk estimate values were examined. The published values were provided to the Environmental

Protection Agency by Oak Ridge National Laboratory (ORNL), and published as Federal Guidance Report 13 , referenced as FGR 13 in the remainder of this document (U.S. Environmental Protection Agency, 2002). FGR 13 provides a risk factor (in terms of risk/Bq) for each nuclide for a given exposure pathway or situation. The values in FGR 13 are based upon ICRP biokinetic models and recommendations for risk factors.

The FGR 13 risk estimates were selected after some deliberation. The concept of assigning risk estimates based upon exposure to radiation implicitly requires assumptions regarding the risk of morbidity (incidence of cancer) or mortality. Entire committees and publications have been devoted to the task of attempting to evaluate risks based upon radiation exposure, or, to oversimplify the task, to convert from the units of |rem|or |Sv| to |%|. As indicated in some published evaluations (Interagency, 2002) FGR 13 risk estimates do not use the most complex method of determining risk factors, but serve as a good way of approximating risks. For this reason, they will be used to estimate risks from the various fission product distributions for comparison only.

Each risk factor is a function of several variables. For a given nuclide, the risk factor is a function of exposure pathway (limited to either ingestion, inhalation, or external exposure in FGR 13), mode or form of exposure (varies by exposure type; for example, for ingestion, either drinking water or dietary), cancer type, age and risk category (either morbidity or mortality for five different age categories).

Thus, to thoroughly examine each fission product distribution a significant amount of assumption (to determine which risk factors are the most relevant or limiting) or computation (to actually evaluate the risks for each fission product distribution) is necessary. In attempt to accommodate both approaches, and receive the benefit of confidence in the evaluation (by means of thorough computation) without spending an enormous amount of effort (by making reasonable assumptions), a hybrid approach was devised.

Initially (at the time step t=0 seconds), all possible cancer types, age and risk categories, and exposure pathways and modes will be evaluated. This requires a significant amount of computation. However, for the time steps after t=0 seconds, only the 'Total' and 'Thyroid' cancer types will be considered. This is based upon the noted health effects from the Chernobyl accident (World Health Organization, 2006), licensing requirements for nuclear reactors, and emergency planning guidance and procedures. Additionally, only the

age categories of 0-5 years (the most limiting age group), and the overall age category of 0-110 years will be evaluated. These assumptions will provide risk estimates for what is credibly the most limiting cancer type in the most limiting age category, while also providing insight for risk estimates to the general population.

Computationally, total risk estimates can be calculated in a straightforward manner. With a given set of assumptions or risk parameters (the above list of exposure pathway, mode, cancer type, and risk and age category), the appropriate risk factor (Bq^{-1}) can be extracted from the FGR 13 data. Multiplying the radionuclide activity found using the methods to calculate radioactivity yields from fission for each fission product nuclide with the appropriate risk factor from FGR 13 produces a risk estimate. The risk estimates for each nuclide in the fission product distribution can be summed to produce a total risk estimate for that radionuclide distribution. An important consideration is that the total risk estimate for each fission product distribution is a function of time, exposure pathway, mode of exposure, cancer type being considered, and the age and risk category. For nuclides that did not have a published risk factor in FGR 13, a null or zero value was used in the overall calculation of risk.

To address all of the needed computations, a series of MATLAB m-files were created to run through the needed calculations. The results were written in MicroSoft Excel spreadsheets to enable efficient data manipulation and summary (such as plotting).

Inhalation Risk Estimates

The inhalation risk factors were used to estimate the relative risks posed by each radionuclide mixture at the time steps mentioned above.

Inhalation risk estimates are tabulated for each nuclide, and are a function of several variables, as mentioned above. However, a primary variable unique to the Inhalation pathway relates to absorption of the nuclide in the body. In FGR 13, risk estimates are tabulated for Fast (F), Medium (M), and Slow (S) absorption types. Each absorption type corresponds to the biokinetics of the radionuclide after entering the body. Additionally, chemical factors influence the behavior of radionuclides in the body after inhalation, and thus have a strong influence on the dose and resulting risk factors. Some nuclides have risk

factors listed for not only F, M, or S absorption types, but additional chemical forms (such as methyl, elemental, or vapor forms).

An appropriate risk factor for each nuclide was selected with a conservative bias, from a risk perspective. Without making assumptions about the chemical form or absorption type of each fission product nuclide, when multiple risk factors for a given nuclide were presented in FGR 13, the greatest risk factor was selected.

Ingestion Risk Estimates

Ingestion risks are further divided into the modes of risk from dietary ingestion, and risks from ingestion through the drinking water pathway. For many nuclides, the risks for these two modes are identical or very similar. However, for some nuclides, due to solubility and absorption, the risks for these two exposure modes differ slightly. Taking this into account, the exposure mode producing the highest risks will be included and analyzed as part of this evaluation.

Obtaining RSAC Results

To further estimate and compare health effects resulting from FP of the MAs with FP of ^{235}U, the Radiological Safety Analysis (RSAC) program was used (Schrader, 2005). This software program models a release of radioactive material to the air, and estimates resulting exposures and doses. The program also provides a radiological decay function and allows the user to address environmental effects, such as buoyancy and atmospheric stability.

To produce a credible result, inputs into the RSAC program were modeled after a historic scenario for fission product exposure. Recently released and analyzed data from Russian atomic testing (Brodsky, 2009) provided an unfortunate, but relevant data point including human effects of fission product exposure. The details of this exposure were incorporated into the RSAC model; most specifically, the distances between the receptors and the point of release of FP.

For the purposes of comparison, an instantaneous release of FP was modeled for each nuclide (Schrader, 2005). The quantity of the release was based upon the activity from

fission, described above. Since the model was intended to serve only as a comparison, the radioactivity data (in units of Bq per fission) was entered as standard RSAC input units, without further conversion.

To acceptably model a release to the environment and obtain risk estimates, several assumptions regarding the fission product distributions for each nuclide were made. First, default RSAC dose conversion factors were assumed, based on ICRP 30 biokinetic models (ICRP, 1979). Although the dose conversion factors from ICRP 30 are not the most recent, they have served the radiation protection community for several decades, are still used by some organizations (for example, the NRC and REACTS), and can be used to provide reasonable estimates of risk for the purposes of comparison.

Secondly, the decay schemes of metastable radionuclide states were simplified. This simplification was necessary to match radionuclides in the existing fission product distributions with listed dose conversion factors. For nuclides that have multiple metastable states listed in either ENDF or NuDat, a single metastable state was assumed. For example, take the nuclide ^{126}Sb. This nuclide has two metastable states as shown in ENDF, NuDat, and other references. However, the listed dose conversion factors in RSAC only recognize one metastable state (Sb-126m). Since metastable states of this nuclide appear as both ^{126m1}Sb and ^{126m2}Sb amongst the FP of several MA and ^{235}U, any occurrences of ^{126m1}Sb and ^{126m2}Sb were each replaced with ^{126m}Sb.

The error introduced by this decay scheme simplification is likely to result in a slight bias of the resulting dose estimates. Depending upon the emissions data incorporated in the RSAC library, neglecting a second excited state of a given nuclide (for example, assuming ^{126m2}Sb is present as ^{126m1}Sb) may neglect the emissions given off by ^{126m2}Sb, and thus ignore the contribution of these emissions to the resulting dose. The end effect is that final dose estimates using simplified decay schemes may be smaller than the actual doses due to the exclusion of some decay and emissions.

The last and most significant assumption for the RSAC analysis related to the FP examined in RSAC. To facilitate the analysis, some nuclides were neglected and excluded from the RSAC input. Obtaining dose or risk estimates following a radionuclide release using RSAC requires dose conversion factors for each nuclide. Without a dose conversion factor (from either the RSAC library or from data input by the user), the model cannot be run, and

results can not be obtained. Many short-lived FP do not have tabulated dose conversion factors listed in the RSAC library, or do not have corresponding radiological decay data in RSAC data library. Similarly, many of these same nuclides do not have dose conversion factors listed elsewhere (such as FGR 11). A list of these nuclides is shown in Appendix F.

Consideration was given to developing dose conversion factors for these nuclides. This task could be undertaken using computational models, compartment modeling software, or extended analytical work and existing decay and biokinetic data for various nuclides and elements. However, the results would need to be validated, most likely by calculating several risk or dose conversion factors using the same methods for nuclides with existing published dose conversion factor or risk data. The overall scope of this task was large enough in nature that it was identified as a recommendation for future work.

Neglecting the contributions from nuclides without dose conversion factors introduced a source of error and uncertainty into this analysis. Clearly these nuclides and their emissions will contribute to not only doses, but also to the in-growth and decay of other radionuclides. Excluding these nuclides from the analysis also introduced a bias into the results; most likely decreasing them from the true values.

Addressing Notation

Throughout the sections described above, the notation used to describe various radionuclides and radionuclide states played a key role in obtaining the best available data and risk estimates. This was particularly relevant because of the multiple data sets and references being used, and often the slightly different notation used in each source.

To establish the best risk estimates and maintain a common form of notation the following methodology was used to describe a given nuclide. First, any isotope (##) of an element (Yy) was described in the traditional manner - $^{##}$Yy, or Yy-## for formatting and computational purposes. Excited states were noted based upon the level of excitation. The first excited state was described as Yy-##m1. The second excited state was described as Yy-##m2, and so on. Other forms of notation described these states sometimes using m, m2, n, or a and b notation.

To help ensure that the notation was properly applied, half-life data from published sources were used as acceptance criteria. When the notation was changed from an 'n,' 'a,' or 'b' to an 'm1', or 'm2;' the half-lives of the nuclide in the data source was cross-referenced with available half-life data (Knolls, 2002, or NNDC) to ensure that the notation was appropriately assigned to a given nuclide.

Treatment of Uncertainty

Throughout each portion of the evaluations described above, several sources of uncertainties were carried through or introduced. ENDF provides fission yield uncertainties for the fission yields examined, while NuDat provides uncertainties for energies and intensities of emissions. Uncertainties for decay constants were not successfully imported from the NuDat database. However, these uncertainties do exist, and can introduce significant errors in some cases (the listed half-life for ^{79}Se in the NuDat database is 2.95E+5 y ± 0.38 E+5y).

Additionally, other sources of uncertainty were introduced into the analysis in the examination of photon exposure rates due to the uncertainties of the mass energy absorption coefficients.

Perhaps the greatest sources of initial uncertainties are tied to the risk estimates. Risk estimates include a variety of uncertainties; the uncertainties associated with biokinetics (Leggett, 2008), the uncertainties associated with age-specific organ masses, and the uncertainties inherent estimating cancer risks from low levels of exposure to ionizing radiation. In addition, the RSAC portion of the analyses above introduced a large uncertainty (or error) by neglecting the nuclides without available decay and dose conversation factor data.

All of the uncertainties in this evaluation were not quantitatively evaluated; many of the uncertainties were not quantified in publication (for example, the uncertainties in the mass energy absorption coefficients). A thorough examination of the uncertainties in this

analysis would require a significant effort, and is included as a recommendation for future work.

Results

Selected results are shown below; with a majority of data publicized elsewhere excluded (decay constants, for example).

Fission Yields by Mass Number

All of the data in this section are based on ENDF information (Chadwick, 2006). As acceptance criteria, the ^{235}U fission yields were compared with well publicized yields for ^{235}U from thermal fission. Several features of the yield curve were found to match existing data, thus providing confidence and assurance in the ENDF results and the processing of the ENDF data.

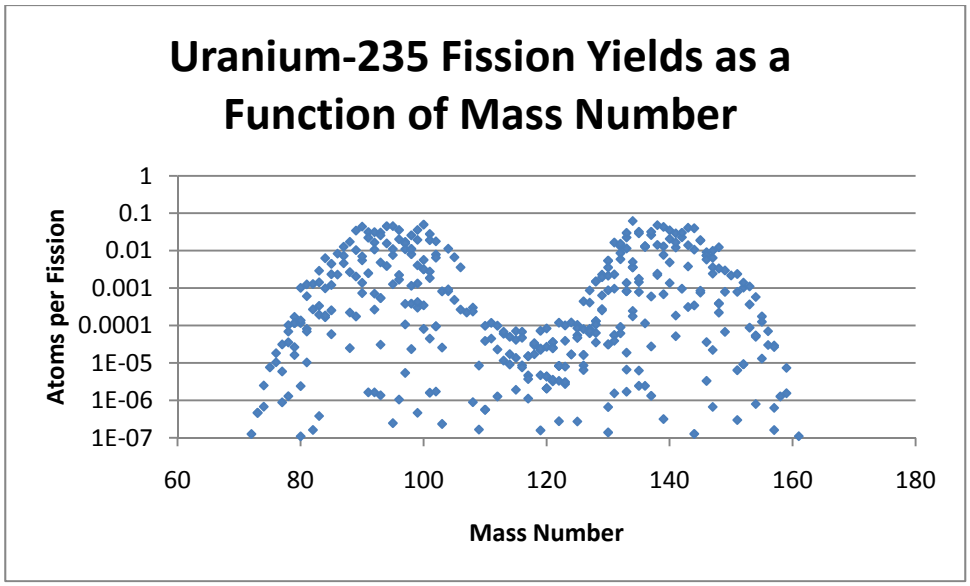

Figure 1. Uranium-235 Fission Yields as a Function of Mass Number. The FP of ^{235}U shown as a distribution of mass numbers, with two identifiable peaks. These results represent the outcome of processing Evaluated Nuclear Data File (Chadwick, 2006) information.

Fission yield data for the FP of other nuclides are shown in Appendix A.

Radioactivity Yields by Mass Number

The activity distributions of FP from each nuclide being evaluated in this study were determined using the methods described above. The results are shown in Appendix B. In general, the distributions show a similar shape to that of the yield distributions. An interesting note is that many of the radioactivity yields show a marked, almost linear slope between mass number 60 and the first relative maximum on the plots.

Activity of Selected Radionuclides

Table 2. Radioactivity from Fission of FRMAC Fission Product Nuclides. The Fission Yields of the nuclides identified by FRMAC are shown below for each nuclide undergoing fission that was considered in this analysis.

Fission Product Nuclide	U-235 (Bq/fission)	Np-237 (Bq/fission)	Am-241 (Bq/fission)	Am-242m (Bq/fission)	Cm-243 (Bq/fission)	Cm-244 (Bq/fission)	Cm-245 (Bq/fission)	Cm-246 (Bq/fission)
Ba-140	3.07E-09	1.59E-09	5.71E-09	3.23E-09	1.56E-08	9.28E-09	3.38E-09	3.07E-09
Ce-141	1.23E-14	1.52E-14	6.52E-13	2.34E-13	4.24E-12	3.93E-12	2.37E-13	1.82E-13
Ce-144	9.73E-12	8.51E-12	3.76E-11	2.95E-11	1.13E-10	8.87E-11	2.01E-11	1.92E-11
Cs-134	4.10E-16	1.35E-15	5.53E-14	2.45E-14	2.41E-13	1.49E-13	1.66E-14	8.93E-15
Cs-136	1.69E-11	3.74E-11	7.82E-10	1.25E-10	1.64E-09	7.16E-10	3.84E-10	1.25E-10
Cs-137	4.38E-13	8.19E-13	3.95E-12	2.52E-12	6.59E-12	6.53E-12	5.43E-12	1.86E-12
I-131	3.91E-11	2.78E-11	2.97E-10	1.43E-10	7.11E-10	3.91E-10	8.12E-11	4.47E-11
I-132	7.66E-09	1.70E-08	9.61E-08	1.03E-07	1.57E-07	1.04E-07	9.12E-08	2.13E-08

Table 2 (Continued). Radioactivity from Fission of FRMAC Fission Product Nuclides. The Fission Yields of the nuclides identified by FRMAC are shown below for each nuclide undergoing fission that was considered in this analysis.

Fission Product Nuclide	U-235 (Bq/fission)	Np-237 (Bq/fission)	Am-241 (Bq/fission)	Am-242m (Bq/fission)	Cm-243 (Bq/fission)	Cm-244 (Bq/fission)	Cm-245 (Bq/fission)	Cm-246 (Bq/fission)
I-133	7.64E-09	1.92E-08	5.04E-08	3.91E-08	6.83E-08	4.53E-08	4.78E-08	1.51E-08
I-134	1.10E-06	2.70E-06	4.14E-06	3.26E-06	4.17E-06	2.91E-06	4.48E-06	1.05E-06
I-135	8.58E-07	1.05E-06	1.09E-06	1.07E-06	8.84E-07	9.69E-07	1.01E-06	7.90E-07
La-140	2.49E-10	4.30E-11	7.31E-10	1.61E-08	2.38E-09	2.08E-09	1.60E-09	2.42E-10
Nb-95	2.43E-13	4.42E-14	5.50E-13	1.55E-13	3.74E-13	1.05E-12	6.43E-11	4.81E-14
Ru-103	4.82E-14	1.26E-13	4.99E-12	1.35E-12	1.81E-11	9.14E-12	1.26E-12	6.09E-13
Ru-106	1.96E-16	1.58E-11	1.31E-10	8.16E-11	2.46E-10	1.70E-10	7.85E-11	4.19E-11
Sb-129	2.80E-08	6.51E-08	2.21E-07	1.65E-07	2.12E-07	1.85E-07	1.06E-07	6.69E-08
Sr-89	2.78E-11	1.78E-12	3.24E-12	2.93E-12	4.60E-12	7.87E-12	8.46E-13	6.41E-13
Sr-90	5.62E-13	1.22E-13	1.71E-13	1.30E-13	1.52E-13	3.02E-13	4.78E-14	3.62E-14
Te-129m1	3.34E-14	6.57E-14	4.75E-11	4.49E-13	8.48E-11	6.15E-11	2.39E-13	1.40E-13
Te-131m1	1.35E-08	1.18E-08	3.87E-08	2.66E-08	6.55E-08	3.25E-08	4.11E-08	1.21E-08
Te-132	3.83E-08	3.80E-08	6.17E-08	5.12E-08	9.31E-08	4.52E-08	4.30E-08	2.34E-08
Xe-135	1.65E-08	4.72E-08	2.31E-07	8.75E-08	3.28E-07	7.45E-08	6.14E-08	1.39E-08
Y-90	1.35E-13	1.90E-13	8.78E-13	5.96E-13	1.05E-12	2.90E-12	1.27E-13	1.18E-13
Y-91	2.26E-13	2.52E-13	8.31E-13	5.66E-13	4.95E-13	1.90E-12	7.34E-14	1.28E-13
Zr-95	1.59E-10	2.98E-11	1.09E-10	4.65E-11	6.03E-11	1.21E-10	1.54E-11	1.54E-11

Radiological Decay

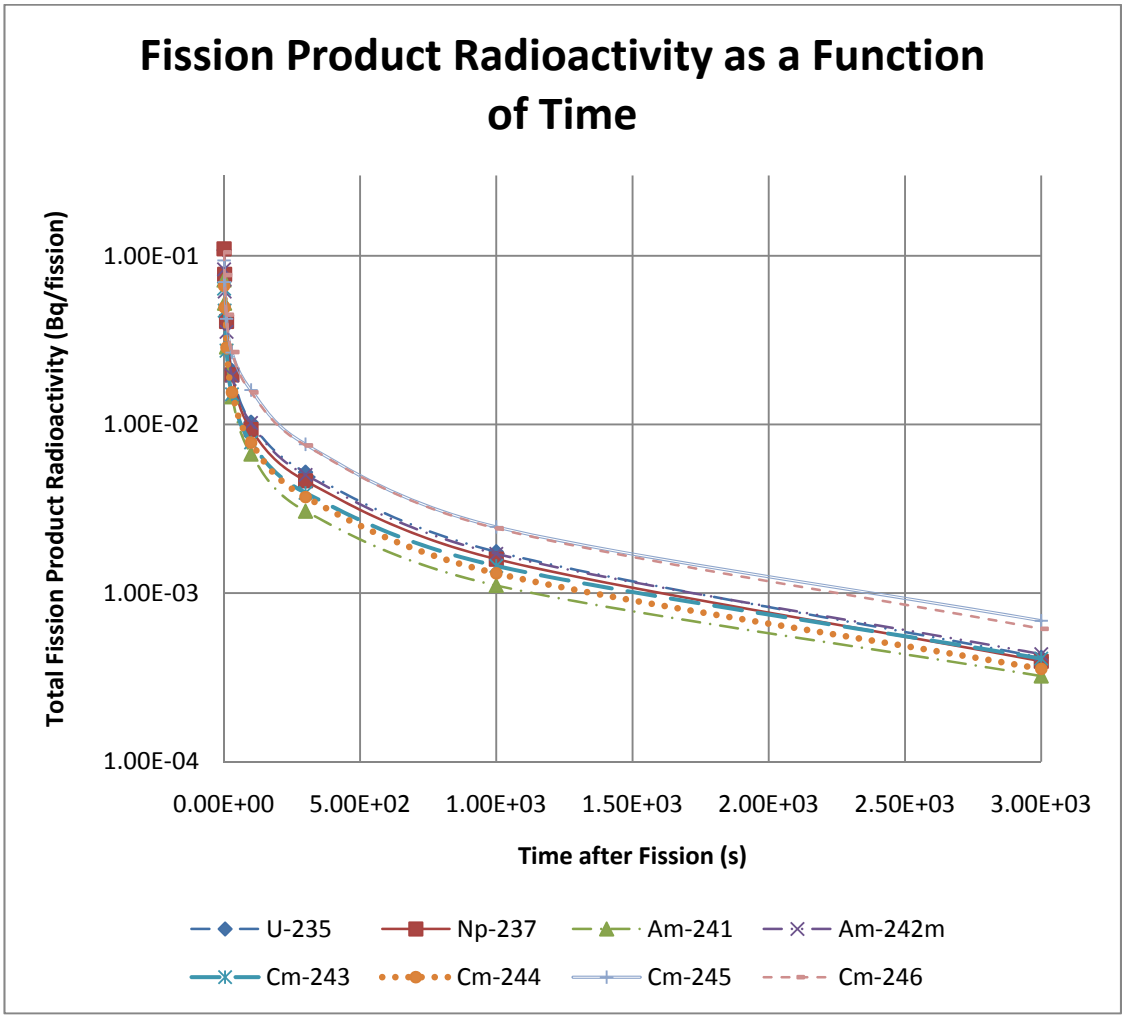

Figure 2. Fission Product Radioactivity as a Function of Time after Fission. The RSAC calculated radiological decay of each fission product mixture is shown. The activities of ^{245,246}Cm are greater than that of the other fission product distributions.

Photon Exposure Rate Estimates by Mass Number

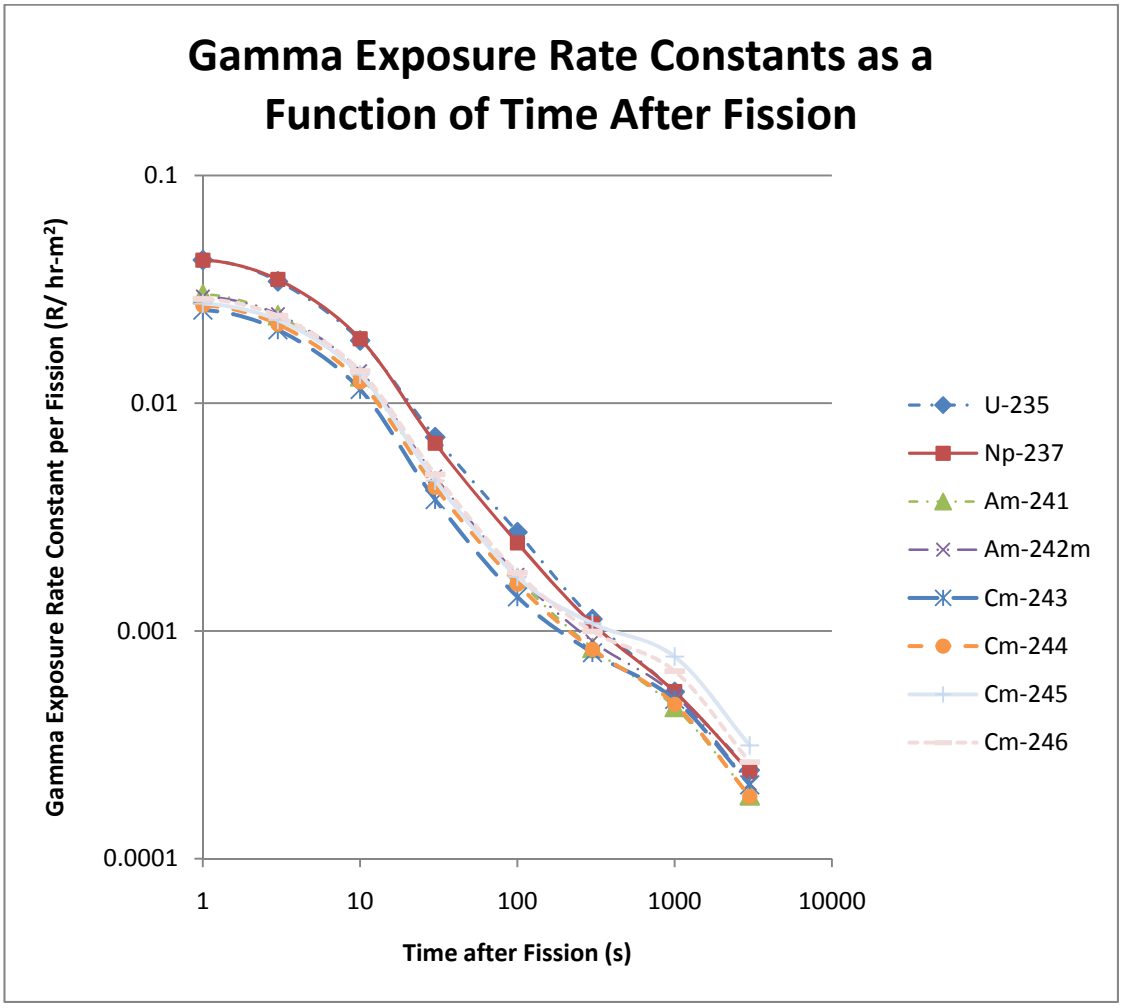

Figure 3. Gamma Exposure Rate Constants as a Function of Time After Fission. As expected, the exposure rates decrease rather rapidly with time, due to the decay of high exposure-rate short-lived radionuclides. The exposure rates from ^{235}U and ^{237}Np FP are greater than those of other fission product distributions until approximately300 seconds. After this time, ^{245,246}Cm FP produce the largest photon exposure rates.

Emitted Energies

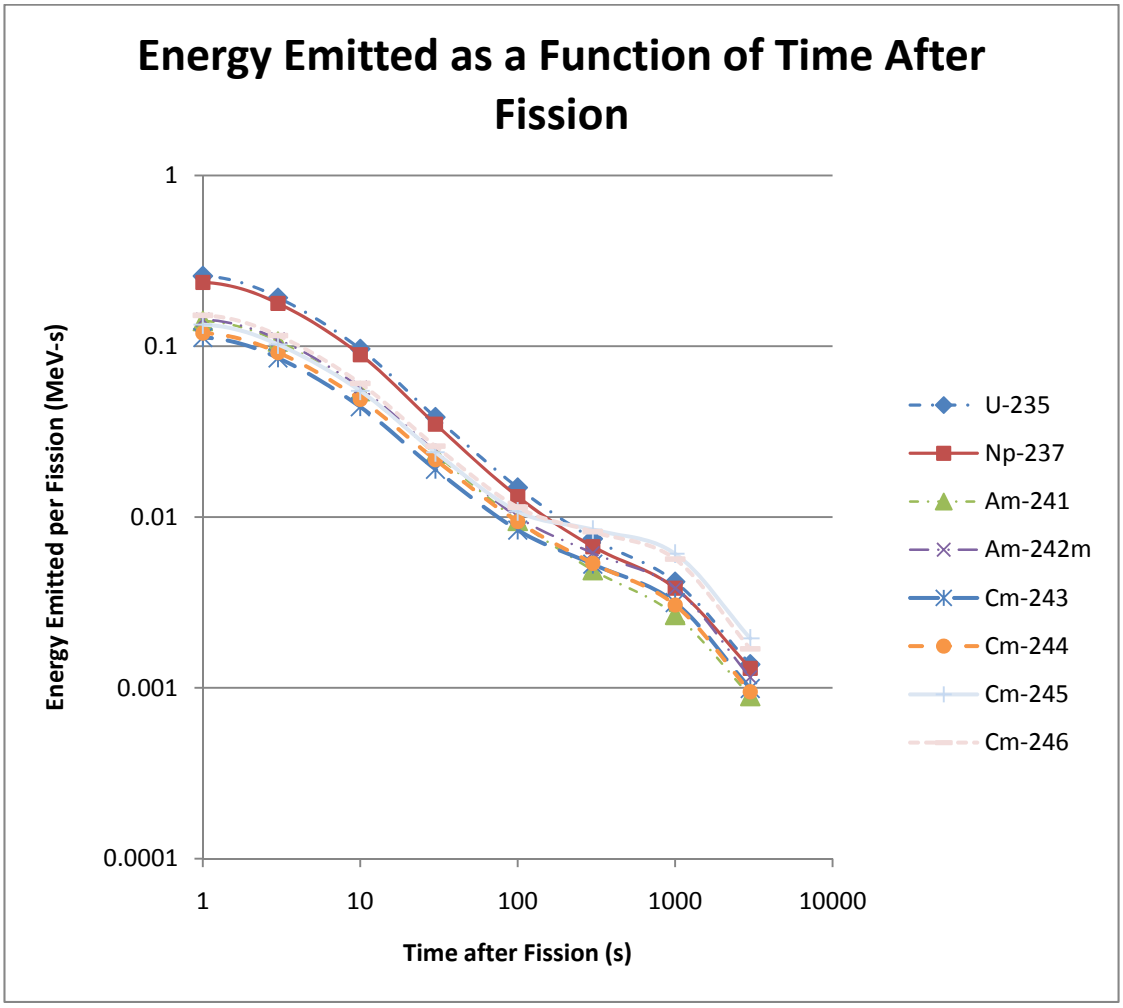

Figure 4. Energy Emitted as a Function of Time after Fission. The total energy emitted from each fission product distribution as a function of time is shown above. The trend exhibited is similar to the trend of photon exposure rates; ^{235}U and ^{237}Np FP emit the most energy up until approximately 300 seconds, after which, the energy emitted from the FP of ^{245}Cm and ^{246}Cm are estimated to be the greatest.

Risk Estimates

Detailed results of the risk estimate evaluations are shown in Appendix E. In general, the risks from FP immediately after fission can be arranged as follows, in decreasing order: ^{241}Am, ^{244}Cm, ^{243}Cm, ^{235}U, ^{242m}Am, ^{237}Np, ^{245}Cm, and ^{246}Cm. The risks of particular cancer types varied by exposure pathway, the source of the FP, and the age of the exposed. In general, the following cancer sites were at the greatest risk: colon, thyroid, lung, stomach, and residual, while the risks for the following cancer types were the smallest: liver, esophagus, kidney, bone, and skin.

The behavior of the risk estimates over time also showed that the maximum risk occurred after the initial fission event. All of the total risk estimates show that maxima occur at approximately 10 seconds after fission. For the thyroid risk estimates, maxima occur at about 1000 seconds after fission.

In general, at any point in time the risks from the FP of ^{241}Am (for times less than 10 seconds after fission), and ^{237}Np and ^{235}U were greater than the risks from the FP of the other nuclides.

RSAC Results

A summary of the RSAC results are plotted below. As described above, the exclusion of the short-lived radionuclides without RSAC data most likely bias these results by slightly decreasing them.

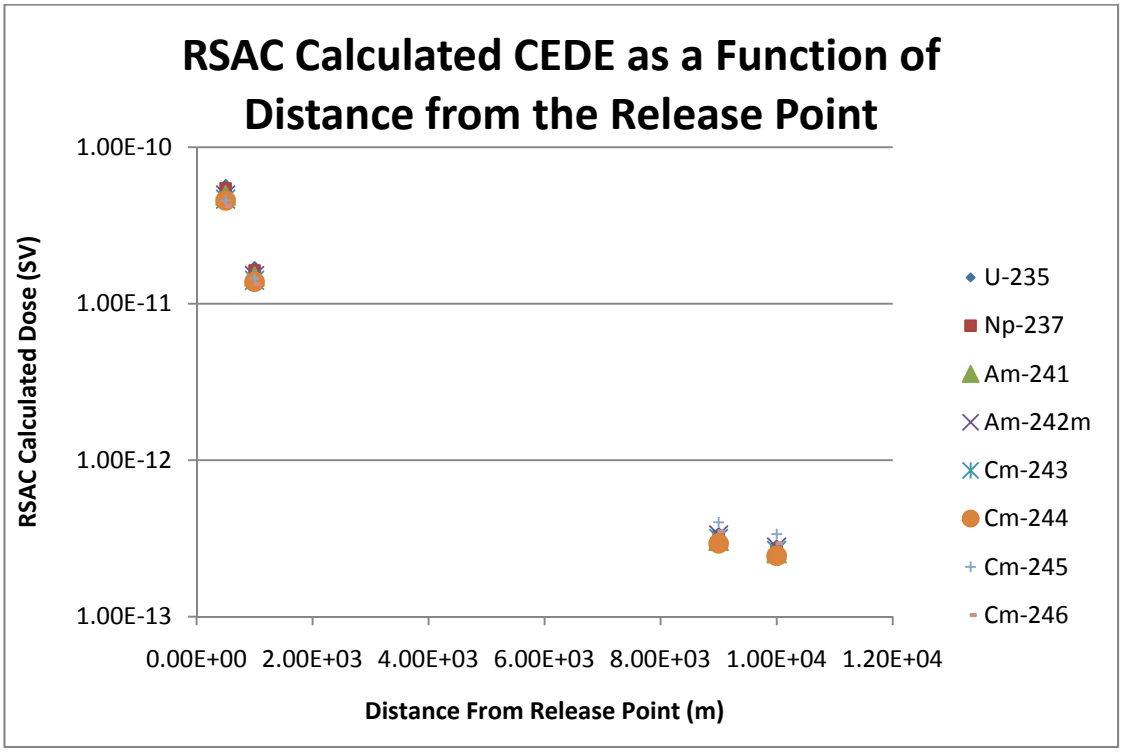

Figure 5. RSAC Calculated CEDEs as a Function of Distance from the Release Point. The RSAC results for an instantaneous release of FP are shown above. The differences in calculated Committed Effective Dose Equivalents (CEDEs) are subtle when illustrated on this scale.

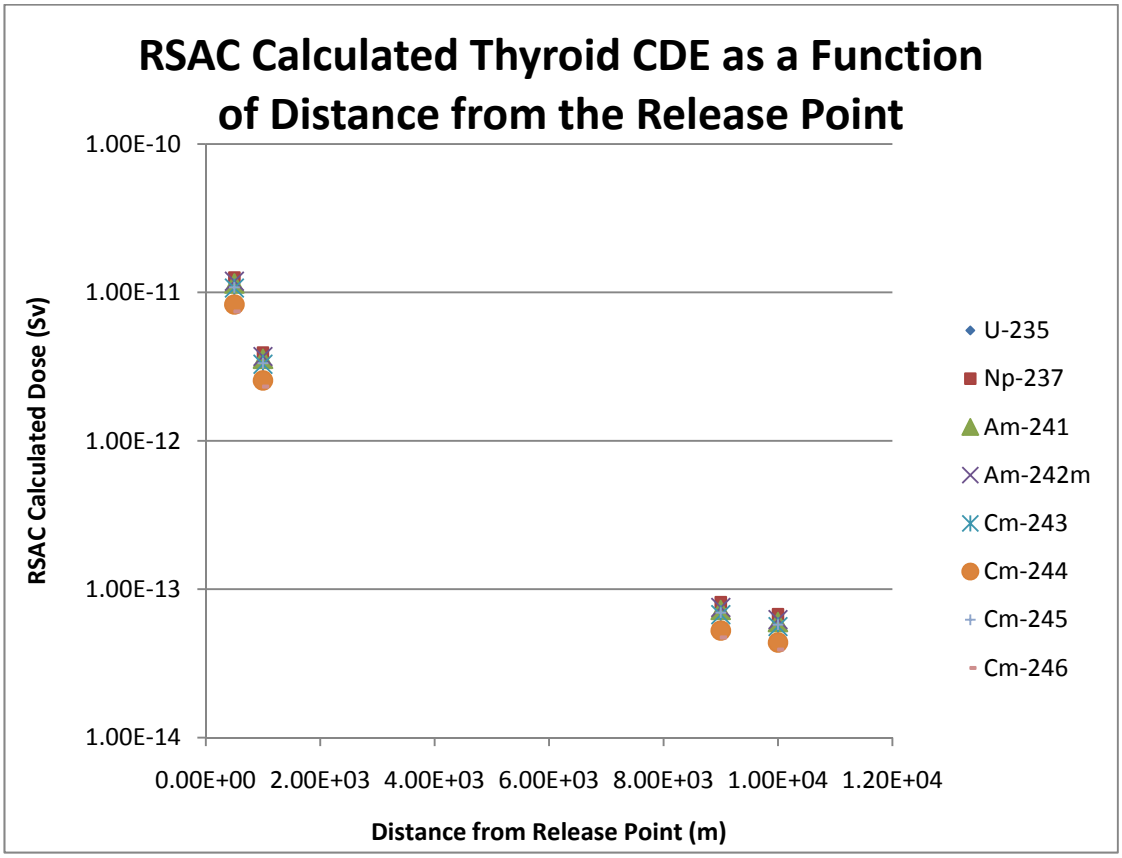

Figure 6. RSAC Calculated Thyroid CDEs as a Function of Distance from the Release Point. The RSAC results for an instantaneous release of FP are shown above. The differences in calculated Thyroid CDEs are subtle when illustrated on this scale, but are less than the calculated CEDEs shown above.

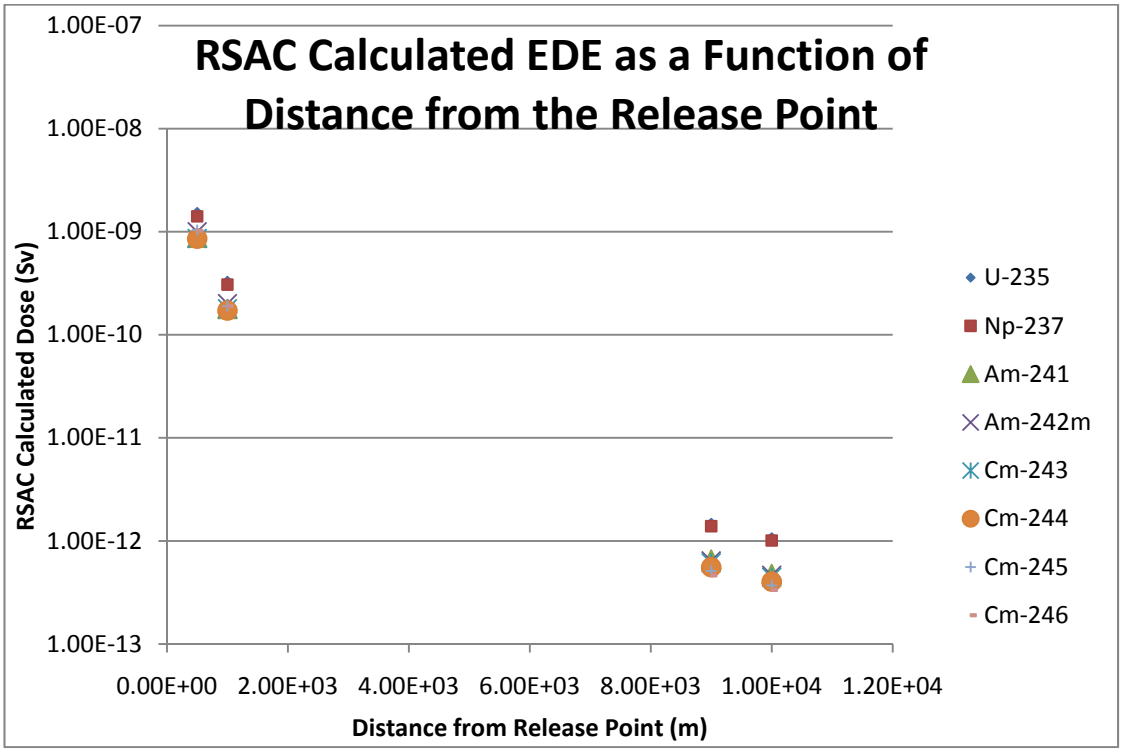

Figure 7. RSAC Calculated EDEs as a Function of Distance from the Release Point. The RSAC results for EDE due to external radiation are shown above. The EDE resulting from ^{237}Np are notably larger than the estimated EDEs from the other nuclides (NOTE: The EDEs calculated for ^{235}U are similar to the ^{237}Np Effective Dose Equivalents (EDEs), but cannot be distinguished in this figure.)

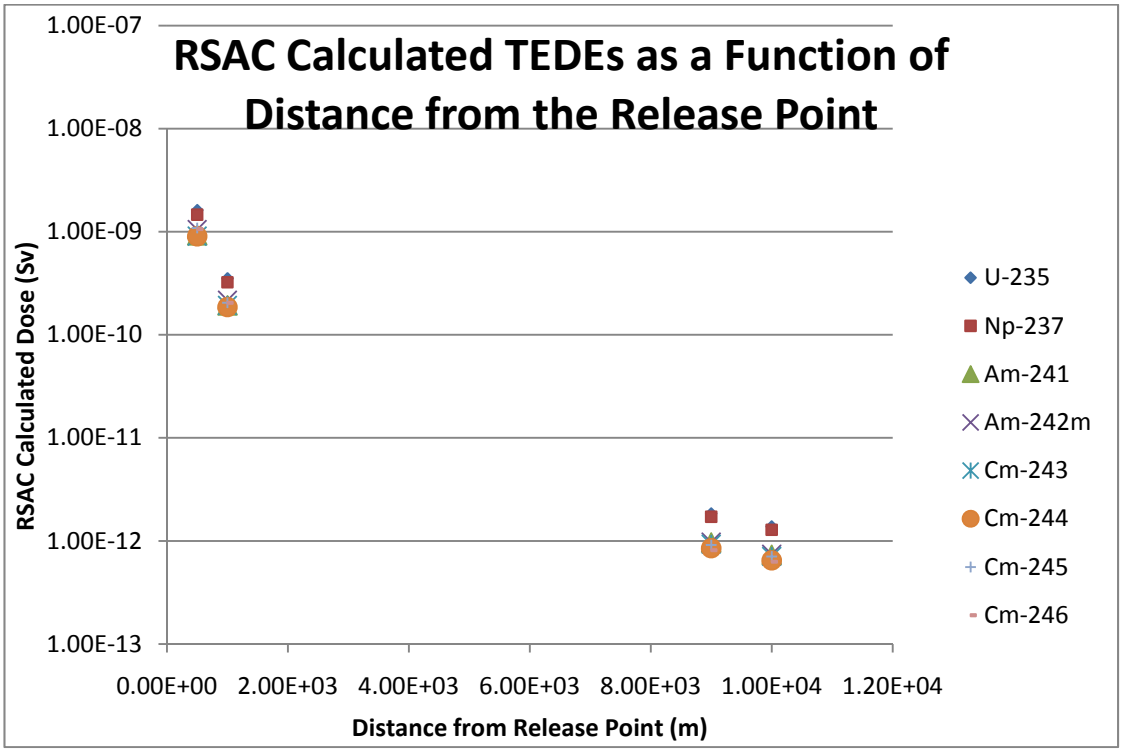

Figure 8. RSAC Calculated TEDEs as a Function of Distance from the Release Point. The results of RSAC calculations for Total Effective Dose Equivalents (TEDEs) are shown above (TEDE = CEDE +EDE). The contribution from EDE for the simulated release scenario is the most significant term.

Discussion

Each of the parameter results above, and contained in the Appendices, will be examined below.

Fission Yields

The fission yields based upon ENDF data seem to agree with published data. Examining the various yield curves, compared to ^{235}U, as the mass number of the nuclide undergoing fission increases, the fission product distribution spreads slightly in mass number, and the difference between the two relative maxima and the trough in between decreases.

Radionuclide Decay

Examining Figure 2 shows that the estimates of fission product activity as a function of time (up to t=3000 seconds or 50 minutes), vary by nuclide undergoing fission. The FP of ^{245}Cm and ^{246}Cm, respectively, are the nuclides with the greatest and second greatest fission product activities after 50 minutes.

Selected Radiouclides

Following the Chernobyl accident in 1986, greater than 90% of the resulting dose to the thyroids of nearby inhabitants was due to ^{132}I exposure through the ingestion pathway (Ron, 2007). Comparing the risks from FP of the selected nuclides, and considering only ^{132}I, the risks posed to the thyroid by ^{243}Cm would be the greatest compared to the FP of other

nuclides. Using this methodology, the FP of ^{235}U are also shown to contain the lowest activity (per fission) of ^{132}I.

This indicates that if significant quantities of MA fuel had been used in the Chernobyl reactor, thyroid doses would have been even greater than what has been observed and estimated in the Ukraine and surrounding areas contaminated by the fallout from that accident. However, as indicated in other sections of this work, the ^{132}I content is affected by the additions from the decay of radioactive parent nuclei. For example, the nuclides ^{132}Te, ^{132}Sb, and ^{132}Sn all eventually decay to ^{132}I. The fission product content of ^{132}I (as a function of time) is then affected by the fission product yields of each of these nuclides. Appendix C contains further information supporting this point. Thus, the content of ^{132}I alone, directly after fission, should not be the only measure used to assess the ingestion risks posed to the thyroid by a given set of FP.

When comparing the fission products of the MAs, there are some of the FRMAC selected radionuclides which are produced in very similar levels from thermal fission (examples include $^{131m1}Te$ and ^{135}I). Other fission product nuclides are produced at very different rates, and may be separated by more than an order of magnitude (for example, based on data in Table 2, thermal fission of ^{243}Cm produces ^{106}Ru at a rate of approximately 10^6 times the production of ^{106}Ru by ^{235}U from thermal fission). Subsequently, ^{106}Ru is identified as one of five radionuclides considered to be a "principal nuclide… expected to deliver the major portion of the radiation dose during the first year" following an accident releasing fission products (DOE, 2007).

Also, ^{132}Tm is identified as the major contributor to external exposure and dose to the bone marrow from plume inhalation (DOE, 2007). Examination of the fission yields of this nuclide shows that the highest production of ^{132}Te results from ^{243}Cm. Another nuclide, ^{131}I, is listed as the primary contributor to ingestion doses at day 7 after a fission product release, and is also shown to be a primary contributor to external exposure, and bone marrow doses from inhalation. Again, the fission products of ^{243}Cm contain the highest quantities of ^{131}I immediately after fission, although quantities of ^{131}I directly after fission varied across only

one order of magnitude. This variation is less significant than variations observed in the quantities of other fission product radionuclides discussed above.

Photon Exposure Rate Estimates

Figure 3 examines the estimated photon exposure rates from the various fission product distributions. The estimates, in conjunction with the RSAC decayed radionuclide distributions, show that the fission product distribution producing the greatest exposure rate will vary with time (between 0 and 50 minutes). Between 0 and 300 seconds, the FP of ^{235}U and ^{237}Np produce the greatest exposure rates, with FP from the other nuclides all producing similar exposure rates. After 300 seconds, the exposure rates from ^{245}Cm and ^{246}Cm FP produce the greatest exposure rates.

In general, the exposure rates decrease sharply as a function of time. Between 1 second after fission and 3000 seconds after fission, the photon exposure rates are estimated to decrease by two orders of magnitude (based upon the radionuclides calculated by RSAC).

Emitted Energies

The energies emitted by the FP as a whole are shown in Figure 4 for each nuclide undergoing fission. This figure incorporates data from the ENDF fission product yields, the NuDat output, and RSAC calculated radionuclide distributions following radiological decay.

In general, the behavior of the energy emitted by the various fission product radionuclide mixtures emulates the behavior of the exposure rates described above. That is, the energy emitted by FP of ^{235}U and ^{237}Np FP are greater than the energies emitted by the FP of the other radionuclide distributions until approximately 300 seconds. After this point, the energies emitted by FP of ^{245}Cm and ^{246}Cm are estimated to be greater.

Risk Estimates

The risk calculations show that ^{241}Am FP produce the highest risk estimates immediately following fission, for ingestion, inhalation, and submersion. This was true of both the 0-5 year and 0-110 year age groups. Using the RSAC decayed radionuclide distributions in conjunction with the FGR 13 risk estimates show that the FP producing the greatest risk vary with time after fission.

For small times after fission, the FP of ^{241}Am produce the greatest risks for inhalation, ingestion, and submersion. Then, between 10 and 100 seconds after fission, the risks posed by FP of ^{237}Np and ^{235}U exceed the risks posed by ^{241}Am FP.

However, an important consideration is noted in the content of FGR 13. As indicated above, there were several radionuclides that did not have published risk factors. For these radionuclides, no contribution to the overall risk was incorporated

The behavior of the risk estimates also show the importance of the build in of progeny radionuclides in a mixtures as time passes. The decay and build-in of radionuclides are responsible for the maxima observed at 10 and 1000 seconds. Significant sources of uncertainty for the risk factors include the lack of risk data for many radionuclides, and the exclusion of nuclides from the RSAC decay analysis.

RSAC Results

EDE RSAC results show that the FP producing the greatest EDE are those of ^{235}U. For CEDE calculations, RSAC estimates that the actinides, and specifically ^{245}Cm, will produce FP that result in the greatest CEDEs.

The RSAC results for thyroid CDE are shown in Figure 6. This figure illustrates the contributions to thyroid dose from the FP of the selected nuclides undergoing fission. An important note is that the FP from ^{237}Np are estimated to produce the greatest thyroid dose, followed by ^{235}U, ^{241}Am, and then the other actinides.

This does not agree with the nuclide evaluation of ^{132}I above. The conclusion is that the RSAC model considers different factors that have significant bearing on the results of the thyroid CDE calculations. These factors most likely include deposition characteristics and the inclusion of other nuclides in the assessment. Perhaps the most significant difference is that the ^{132}I discussion above is based largely on ingestion dose following the Chernobyl accident. The RSAC model created above considers only inhalation (CEDEs) and external exposure due to gamma emissions from the resulting cloud (EDE). No assumptions regarding ingestion exposure pathways were made in the RSAC model since the doses from this pathway are often geographically, culturally, and seasonally specific.

Summary

In general, the risks posed by FP of one particular nuclide did not produce exposure rates, risk estimates, or dose estimates that were greater than the other nuclides. The FP producing the greatest exposure rates, the most energetic emissions, the largest risk, or the highest dose varied with the time after fission, the parameter being examined, and the assumptions being used.

There were many situations where ^{235}U FP were the greatest radiological insult. However, FP from ^{237}Np were a significant concern in several cases, and appeared to be most akin to the ^{235}U FP frequently encountered. This conclusion is somewhat intuitive, since the mass numbers of ^{235}U and ^{237}Np are most alike. The radionuclide yields from ^{243}Cm immediately following fission show greater quantities of radiotoxic nuclides of interest, such as ^{106}Ru, ^{131}I, ^{132}I, and ^{132}Te. The FP of ^{241}Am may be a limiting concern at times between 0 and 10 seconds after fission based upon risk estimates. The MA s ^{245}Cm and ^{246}Cm are estimated to present additional risks at times after 300 seconds. In addition, the RSAC analyses of the FP of ^{245}Cm and ^{246}Cm indicate that their contribution to thyroid doses may be greater than contributions to the thyroid from the FP of other nuclides following a radiological release.

Table 3. Summary of Evaluations. The various evaluations conducted in this paper and the original nucleus whose FP produced the highest estimated risk for each parameter of interest are shown.

	Parameter	Nuclide Producing Fission Products with the Greatest Risk Estimates and Other Results
Radioactivity Evaluations	Total Radioactivity	^{245}Cm for times from 30 seconds to 50 minutes after fission.
	^{90}Sr Radioactivity	^{235}U
	^{132}I Radioactivity	^{243}Cm
	^{137}Cs Radioactivity	Very similar results for all fission product distributions.
	Photon Exposure Rates	^{237}Np and ^{235}U for times between 0 and 300 seconds; ^{245}Cm for times between 300 and 3000 seconds.
	Energy Emitted	^{237}Np at time 0, ^{235}U for times between 1 and 300 seconds; ^{245}Cm for times of 300 to 3000 seconds.
Risk Estimates	Inhalation Risks (Total)	^{241}Am for times 0 to 10 seconds, ^{235}U for times 10 seconds to 50 minutes.
	Ingestion Risks (Total)	^{241}Am for times 0 to 10 seconds, ^{235}U for times 10 seconds to 50 minutes.
	Submersion Risks (Total)	^{241}Am for times 0 to 10 seconds, ^{235}U for times 10 seconds to 50 minutes.
RSAC Release Evaluations	RSAC Calculated CEDE	^{245}Cm
	RSAC Calculated Thyroid CDE	^{237}Np
	RSAC Calculated EDE	^{235}U
	RSAC Calculated TEDE	^{235}U (mostly driven by EDE)

Recommendations

This work was able to identify several subjects that would benefit from receiving further attention and research. First, several nuclides identified by ENDF as constituting a portion of the fission product yields of each radionuclide were lacking corresponding decay data or emissions data. The nuclide ^{66}V is an excellent example of one such nuclide. Other nuclides, many of which are short lived, were lacking dose conversion factors in ICRP 30 or risk factors in FGR 13. Further research to identify the emissions and decay data for the first set of nuclides, and to estimate the biokinetics and resulting risk from the second group of nuclides would be a benefit to the scientific community.

Additionally, due to the variety of data sets used, several notation differences were identified. A universal set of notations for describing radionuclides would prevent these inconsistencies. Consistency gains could also be realized in identifying the most relevant radiological decay data sets. In this paper, decay data from NuDat2 were used, assuming this database contained the most up-to-date radiological information. Near the time of the publication of this report, the ICRP published updated decay data for use in radiological and dosimetric assessment (ICRP, 2009). The availability of multiple sets of data (not all of which are consistent), without a single set identified as the standard, creates a trap for researchers and scientists.

As mentioned above, uncertainties were not addressed in this evaluation. The uncertainties and statistical error in the results of this work could significantly affect the conclusions drawn, and should be evaluated and characterized. Also, the wide variance in the listed half-life for ^{79}Se underscores the need for further work understanding the effects of half-life uncertainties on dose and risk estimate results.

Further research could also be done to address the effects of incident neutron energy on the health risks of FP. Only thermal neutron energies were evaluated in this paper; however, some concepts for new nuclear reactors being put forward incorporate a fast neutron spectrum.

Following this evaluation there is more than ample room for additional research. The external photon exposure rates examined were those resulting from a point source in air. Additional relevant geometries could include cylinders and cuboids with thin layers of zirconium cladding. Technologically sophisticated software, such as MCNP or ORIGEN could also be used to evaluate the various fission product mixtures.

Conclusion

Using a method of only examining specific radionuclides following fission could be misleading. Take the conclusions that were reached based upon nuclides highlighted as important following a Light Water Accident in the FRMAC Manual (DOE, 2007). Many of these conclusions support the claim that the risks from the FP of ^{243}Cm are greater than the risks from FP of other radionuclides. Now examine the results of the other evaluations. Fission products of ^{243}Cm do not show up as a limiting or primary contributor to risk. This does not rule out the possibility that ^{243}Cm FP could be the most limiting at times greater than 50 minutes following fission; however, the discrepancy does illustrate that each fission product radionuclide distribution must be viewed as a unique collection of individual nuclides.

The health risks from FP of the MAs are estimated to be greater than the health risks from the FP of ^{235}U in several cases. Based only on radionuclide yields, ^{243}Cm FP are estimated to produce the greatest risks. However, other evaluations show that, in some cases, FP from ^{237}Np, ^{241}Am, ^{245}Cm, and ^{246}Cm produce either dose rates or risk estimates greater than those of ^{235}U fission products. Additionally, the risk estimates show that inhalation of FP in the limiting age group (0-5 years) results in a significant risk to the colon – a risk greater than the risks to the lung, and even greater than the risk to the thyroid from some fission product distributions.

Bibliography

Baetsl, L.H. (1997) Some aspects of risk reduction strategy by multiple recycling in fast burner reactors of the plutonium and minor actinide inventories, *Nuclear Engineering and Design, 197*, 359-366

Beck, H.L., Krey, P.W. (1983), Radiation exposures in Utah from Nevada nuclear tests, *Science*, *220*(4592), 18-24

Bergelson, B. R., Gerasimov, A. S., Kiselev, G. V., Tikhomirov, G. V. (2004), Efficiency of preliminary transmutation of actinides before ultimate storage, *Nuclear Engineering and Design, 230*, 333-338

Brodsky, A., Reeves, G (2009), New Human Data versus Estimates of Effects of Inhaling Fission Product Mixtures, *Health Physics*, *96*(1), 1-4

Carbol, P., Solatie, D., Erdmann, N., Nylen, T., Betti, M. (2003), Deposition and distribution of Chernobyl fallout fission products and actinides in a Russian soil profile, *Journal of Environmental Radioactivity, 68*(1), 27-46

Cember, H. (1996), *Introduction to Health Physics, Third edition*, New York, NY: McGraw-Hill

Chadwick, M.B., Oblozinsky, P., Herman, M., Greene ,N.M., McKnight, R.D., Smith, D.L., et al (2006), ENDF/B-VII.0: Next Generation Evaluated Nuclear Data Library for Nuclear Science and Technology, *Nuclear Data Sheets*, *107*, 2931-3060.

Englad, T.R., Rider, B.F. (1995), *Evaluation and compilation of fission product yields*, (LA-UR-94-3106).

Forsberg, C. (2000), Disposal of partitioning-transmutation wastes with separate management of high-heat radionuclides (^{90}Sr and ^{137}Cs) from: *6th Informational Exchange Meeting on Actinide and Fission Product Partitioning And Nuclear Waste Transmutation Organization for Economic Cooperation and Development:* Nuclear Energy Agency, Madrid, Spain

Gurion, Ben (2001). Extremely Efficient Nuclear Fuel Could Take Man To Mars In Just Two Weeks, *ScienceDaily*. Retrieved March 24, 2009, from http://www.sciencedaily.com /releases/2001/01/010103073253.htm

Interagency Steering Committee on Radiation Standards (2002), *A Method for Estimating Radiation Risk from Total Effective Dose Equivalent (TEDE)* (ISCORS Technical Report 2002-02) Washington, D.C.

International Commission on Radiological Protection (1979), *Limits for Intakes of Radionuclides by Workers, Part 1,* (ICRP Publication 30), Pergamon Press, Oxford, Great Britain.

International Commission on Radiological Protection (1983), Radionuclide Transformations, Energy and Intensity of Emissions,(ICRP Publication 38), Pergamon Press, Oxford, Great Britain

International Commission on Radiological Protection (2009), Nuclear Decay Data for Dosimetric Calculations,(ICRP Publication 107), Elsevier.

Ivanova, N.V., Shvydko, N.S., Ershov, E.B., Balonov, M.I. (1995), Population Doses in Russia from Plutonium Fallout Following the Chernobyl Accident, *Radiation Protection Dosimetry, 58*, 255-260

Knolls Atomic Power Laboratory (2002), *Chart of Nuclides 16th Edition*, Lockheed Martin Corporation.

Leggett, R. W., Eckerman, K. F., Meck, R. F. (2008), *Reliability of Current Biokinetic and Dosimetric Models for Radionuclides: A Pilot Stud*y, (Oak Ridge National Laboratory ORNL/TM-2008/131) Oak Ridge, TN

National Nuclear Data Center, information extracted from the NuDat 2 database, http://www.nndc.bnl.gov/NuDat2/

Osaka, M., Koyama, S., Mitsugashira, T (2004), Analysis of curium isotopes in mixed oxide fuel irradiated in fast reactor, *Journal of Nuclear Science and Technology*, *41*(9), 907-914

Renaud, P., Louvat, D. (2004), Magnitude of fission product deposition from atmospheric nuclear weapon test fallout in France, *Health Physics, 86*(4), 353-358

Ron, E. (2007), Thyroid Cancer Incidence Among People Living in Areas Contaminated by Radiation from the Chernobyl Accident, *Health Physics*, *93*(5), 502-511

Sahin, S., Kumar, A. (1984), Fast hybrid thermionic blankets with actinide waste fuel, *Journal of Nuclear Technology/Fusion, 5*(3), 374-381

Sasahara, A., Matsumura, T., Nicolaou, G., Papaioannou, D. (2004), Neutron and Gamma Ray Source Evaluation of LWR High Burn-up UO2 and MOX Spent Fuels, *Journal of Nuclear Science and Technology, 41*(4), 448-456

Schrader, B. J. (2005), *RSAC 6.2 with WinRP 2.0 User Manual*, (INL/EXT-05-00642), Idaho National Laboratory, Idaho Falls, Idaho.

Shinohara, N., Hatsukawa, Y., Hata, K., Kohno, N. (1999), Measurement of fission product yields from neutron-Induced fission of Americium-241, *Journal of Nuclear Science and Technology*, *36*(3), 232-241

Shultis, J.K., Faw, R.E. (1999), *Radiological Assessment: Sources and Doses*, La Grange Park, IL: American Nuclear Society

Shultis, J.K., Faw, R.E. (2000), *Radiation Shielding*, La Grange Park, IL: American Nuclear Society

Stabin, M.G., da Luz, L (2002), New Decay Data for Internal and External Dose Assessment, *Health Physics, 83*(4), 471-475.

U.S. Department of Energy, (2007) *FRMAC Assessment Manual, Volume 3 - Pre-assessed Default Scenarios* (SAND2003-1073P) Las Vegas, NV

U.S. Environmental Protection Agency (1999) *Cancer Risk Coefficients for Environmental Exposure to Radionuclides*. (Federal Guidance Report No. 13. EPA 402-R-99-001), Washington, DC.

U.S. Environmental Protection Agency (April 2002) *CD Supplement, Rev. 1: Cancer Risk Coefficients for Environmental Exposure to Radionuclides*. (Federal Guidance Report 13 EPA 402-C-99-001,Rev. 1), Washington, DC.

von Hippel, F. N. (2001), Plutonium and Reprocessing of Spent Nuclear Fuel, *Science*, *293*(5539), 2397-2398

Westlén, Daniel (2007), Reducing radiotoxicity in the long run, *Progress in Nuclear Energy, 49*(8), 597-605

World Health Organization (2006), *Health Effects of the Chernobyl Accident and Special Health Care Programmes,* Geneva

World Nuclear Association (2009), *Mixed Oxide (MOX) Fuel*, Retrieved March 2009 from http://www.world-nuclear.org/info/inf29.html

Wright, R. Q., Hopper, C. M. (2008), Calculation of the minimum critical mass of fissile nuclides, *Nuclear Science and Engineering*, *158*(2) 203-209

Yoga Peryoga, Masaki Saito, Hiroshi Sagara (2005), Improvement of plutonium proliferation resistance by doping minor actinides" *Progress in Nuclear Energy*, *47*(4), 693-700

APPENDICES

Appendix A: Fission Yield Data

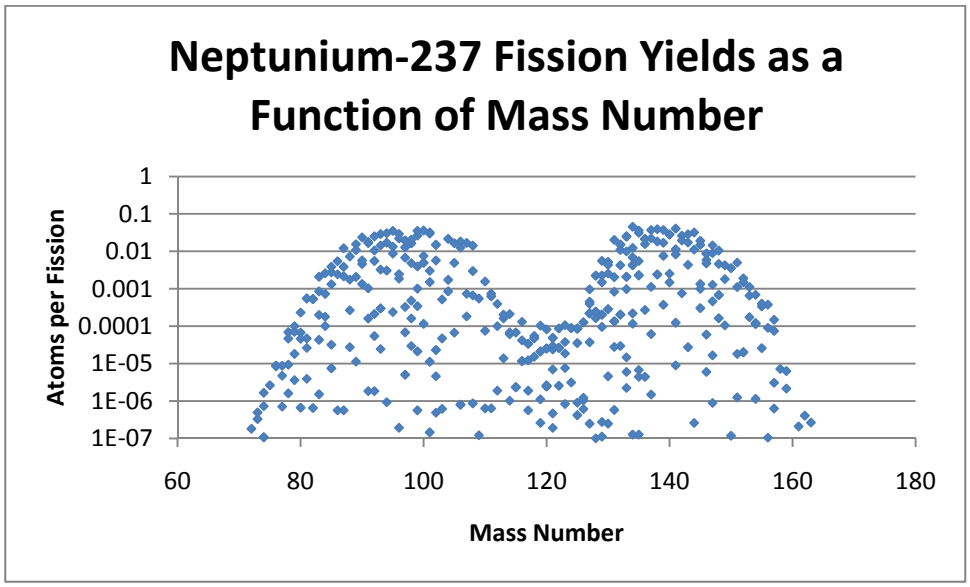

Figure A.1. Neptunium-237 Fission Yields as a Function of Mass Number. The fission product distribution of ^{237}Np is similar to the ^{235}U fission product distribution shown in Figure 1, with slightly smaller relative maxima (at mass numbers of approximately 95 and 140).

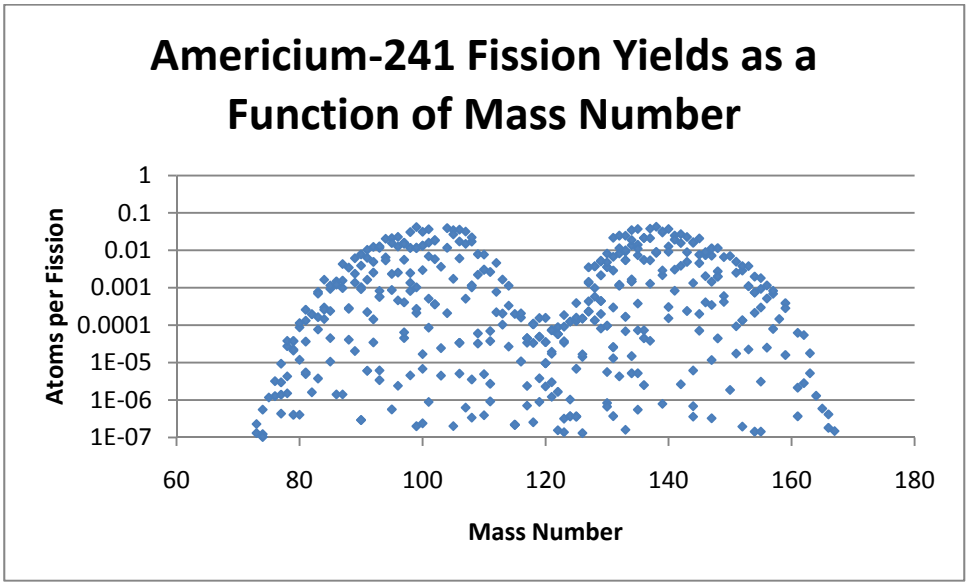

Figure A.2. Americium-241 Fission Yields as a Function of Mass Number. The fission product distribution of ^{241}Am is shown.

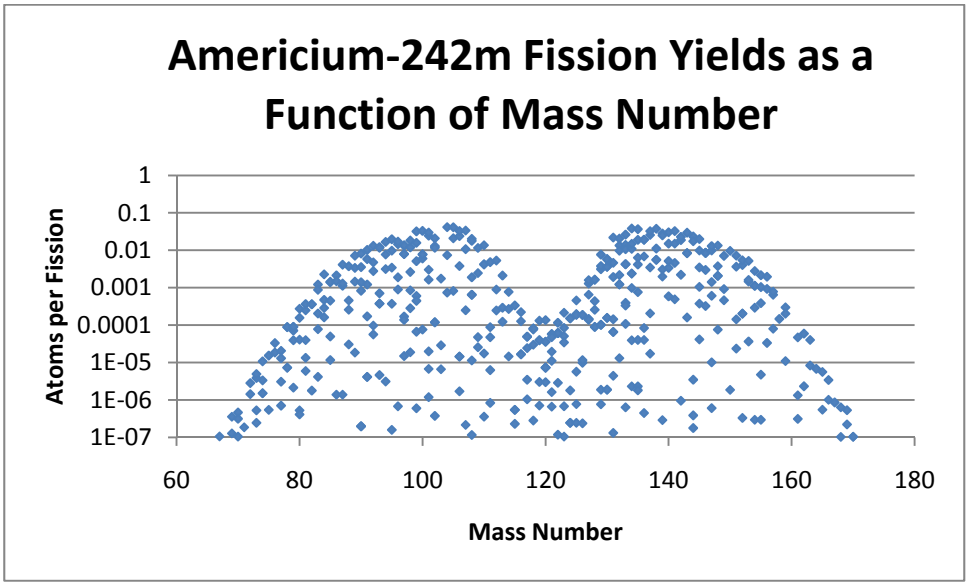

Figure A.3. Americium-242m Fission Yields as a Function of Mass Number. The ^{242m}Am fission product distribution continues the trend exhibited by ^{237}Np and ^{241}Am; the distribution becomes broader in mass number, with slightly smaller values of the relative maxima.

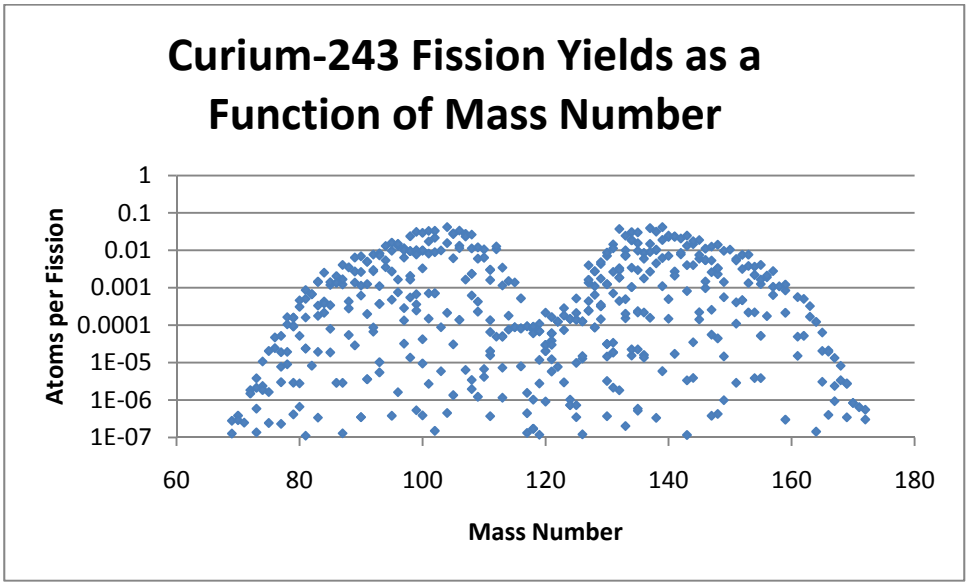

Figure A.4. Curium-243 Fission Yields as a Function of Mass Number. The fission product distribution of ^{243}Cm is very similar to the fission product distribution of ^{242M}Am shown above.

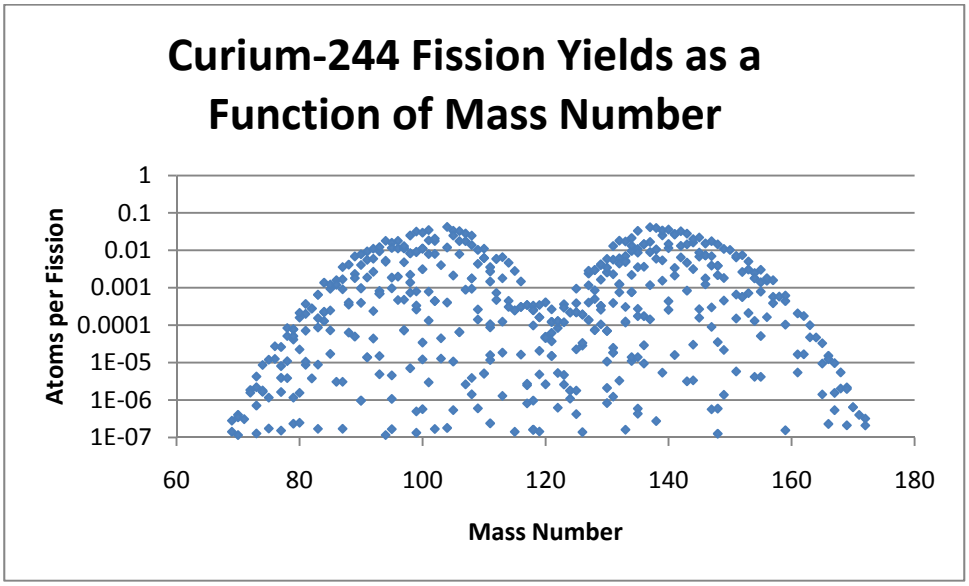

Figure A.5. Curium-244 Fission Yields as a Function of Mass Number. The fission yields of ^{244}Cm exhibit differences from the ^{235}U fission yields. Most notably, the difference between the values of the relative maximum and the relative minima (at mass numbers of about 105 and 120, respectively) are less than two orders of magnitude.

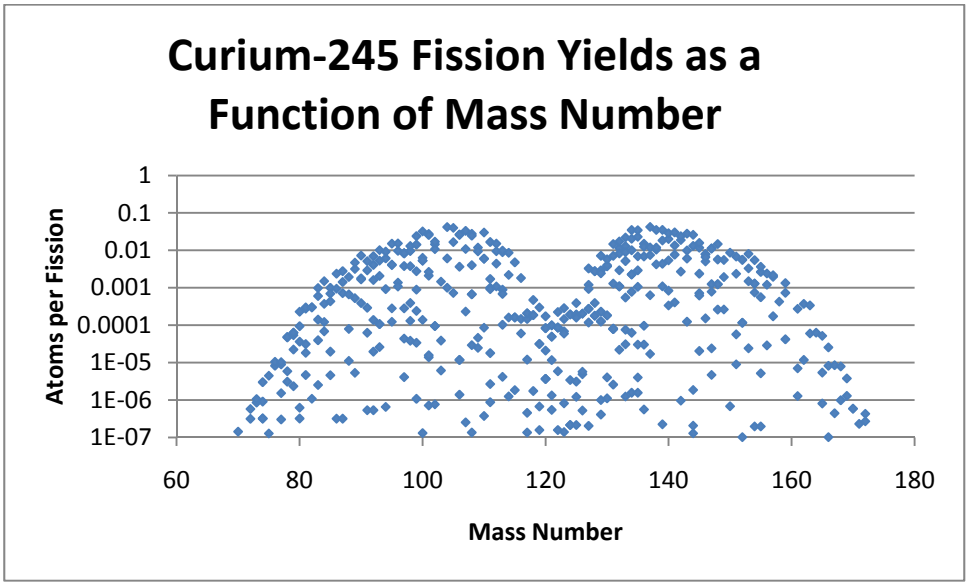

Figure A.6. Curium-245 Fission Yields as a Function of Mass Number. The ^{245}Cm fission yields, which appear very similar to the ^{244}Cm fission yields are shown.

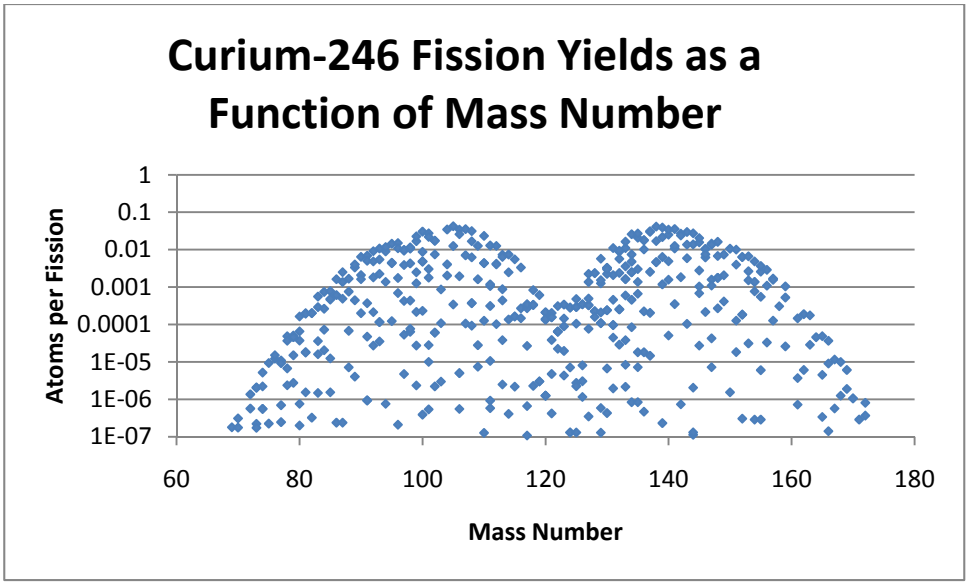

Figure A.7. Curium-246 Fission Yields as a Function of Mass Number. Fission yields of the nuclide with the greatest mass number examined in this study (^{246}Cm) are shown. Compared with Figure 1, the distribution is broader, with slightly less pronounced maxima, and a less severe relative minimum.

Appendix B: Radioactivity Yields from Fission

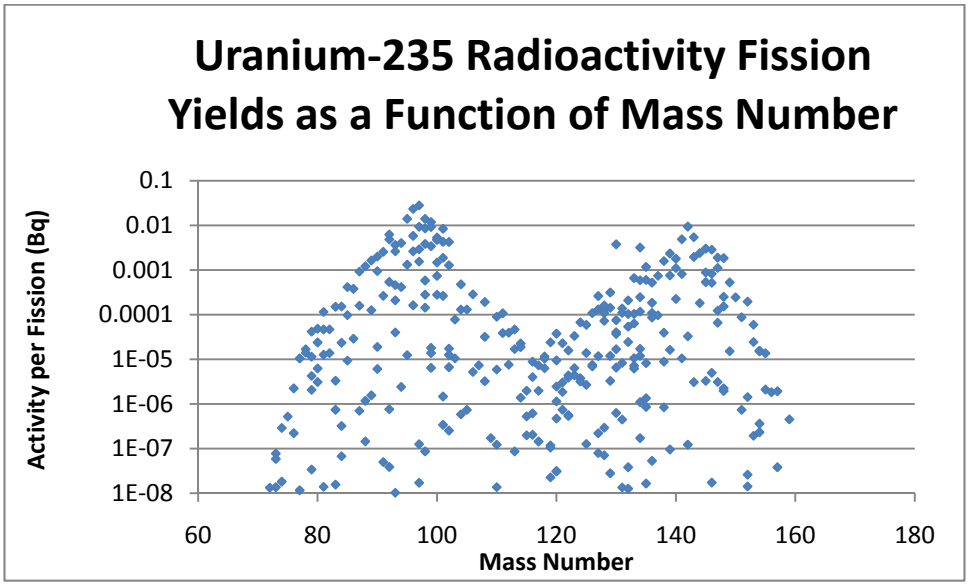

Figure B.1. Uranium-235 Radioactivity Yields as a Function of Mass Number.

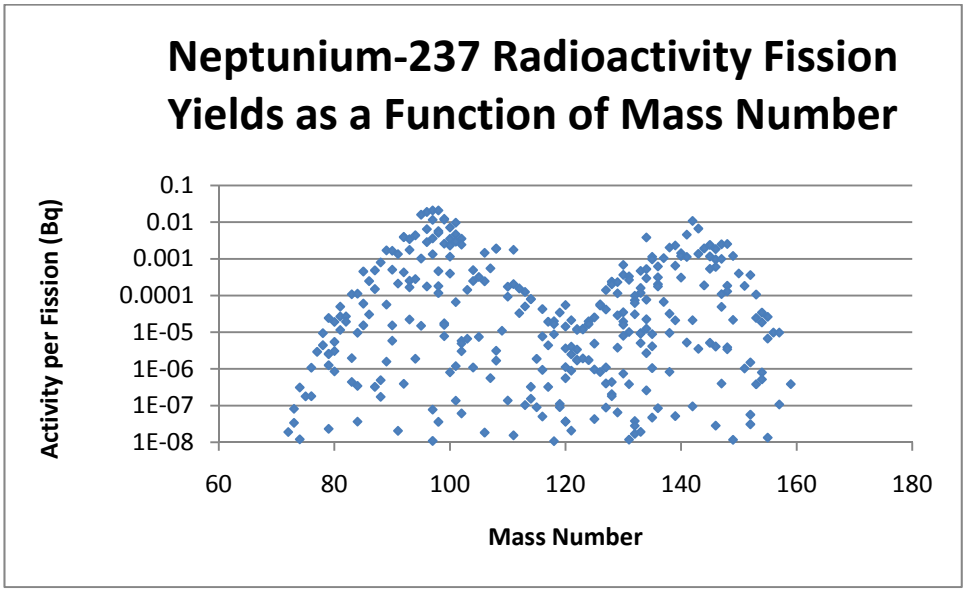

FigureB.2. Neptunium-237 Radioactivity Yields as a Function of Mass Number.

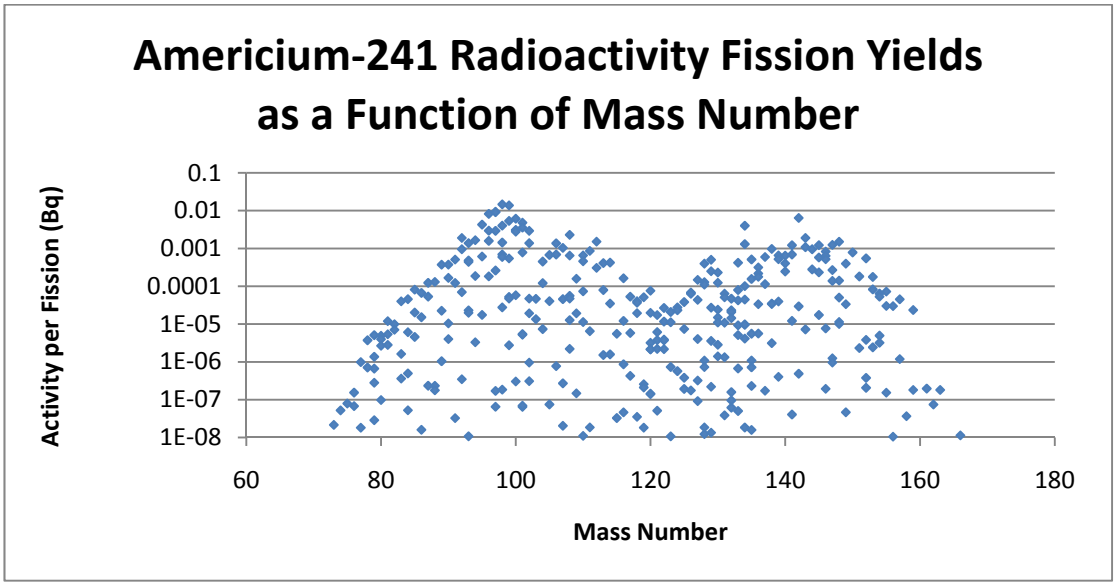

Figure B.3. Americium-241 Radioactivity Yields as a Function of Mass Number.

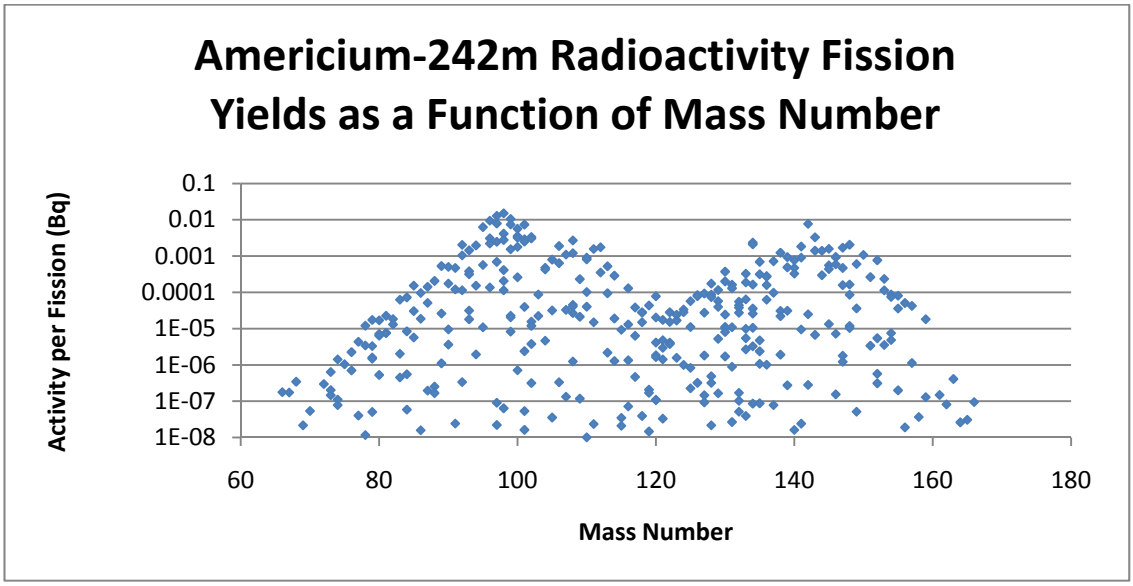

Figure B.4. Americium-242m Radioactivity Yields as a Function of Mass Number.

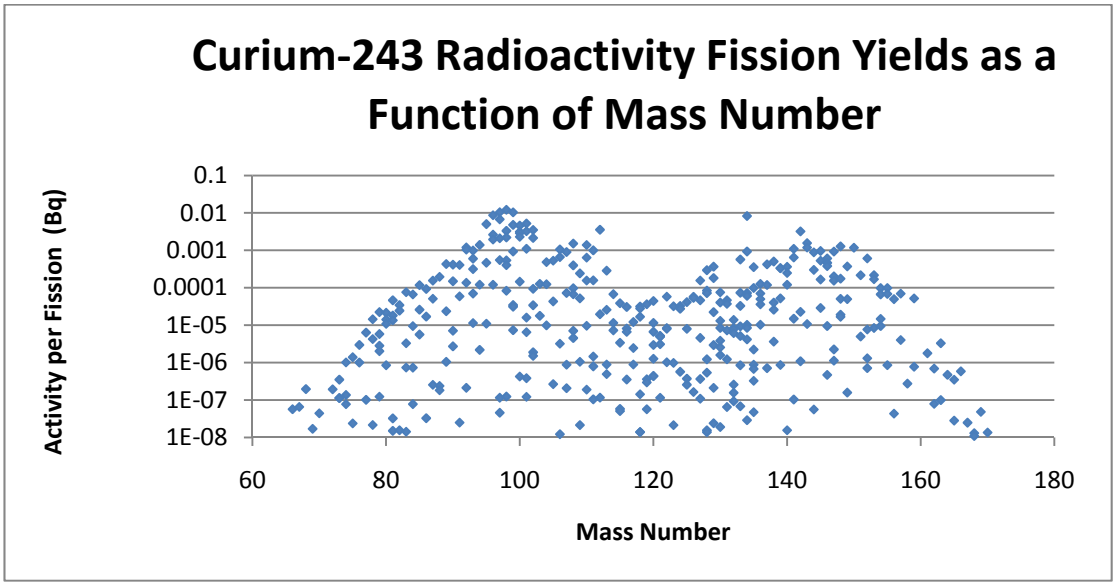

Figure B.5. Curium-243 Radioactivity Yields as a Function of Mass Number.

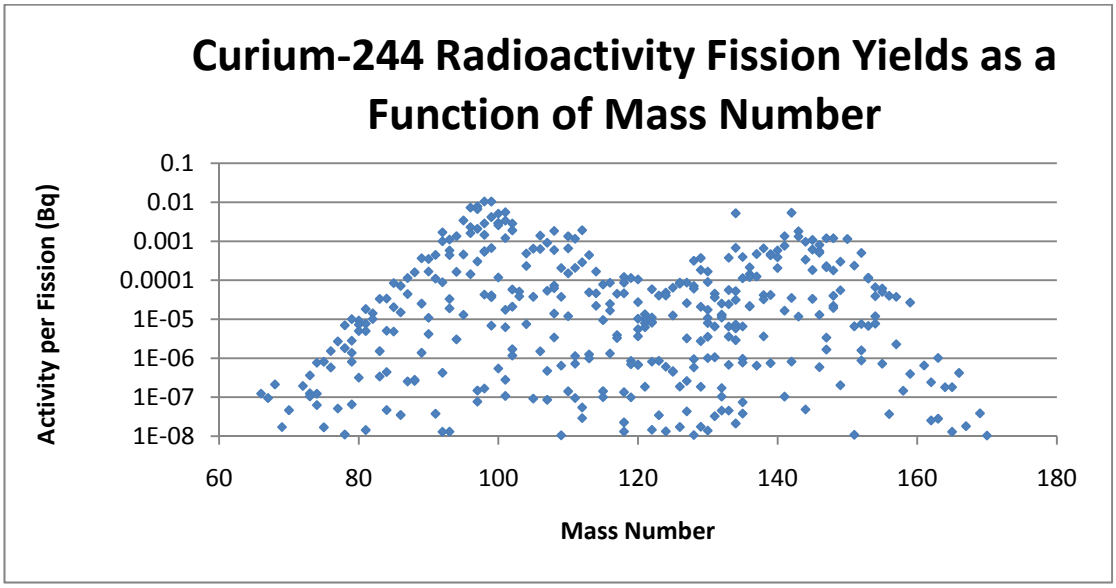

Figure B.6. Curium-244 Radioactivity Yields as a Function of Mass Number.

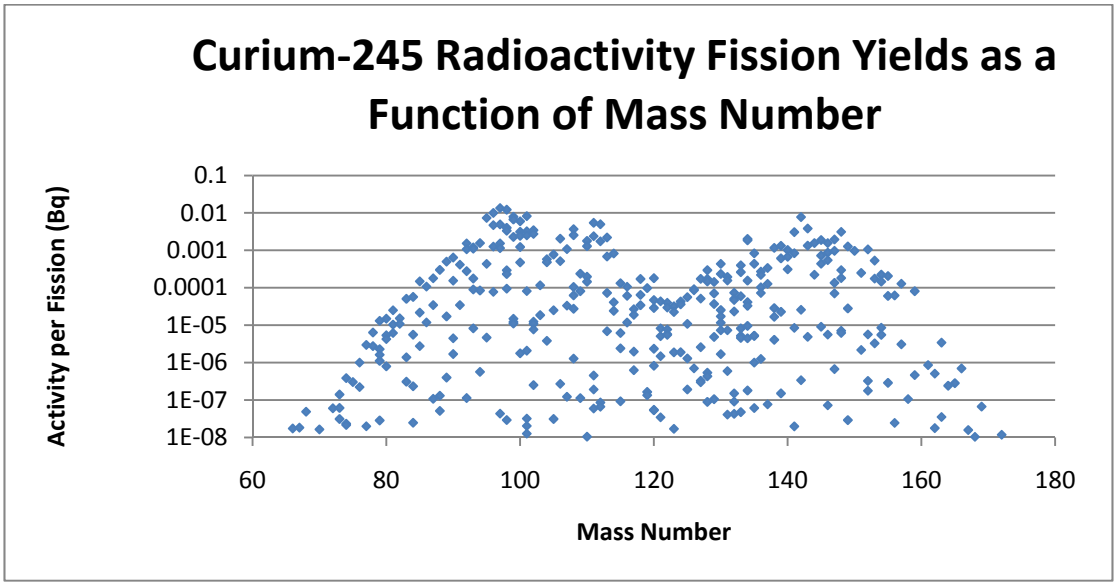

FigureB.7. Curium-245 Radioactivity Yields as a Function of Mass Number.

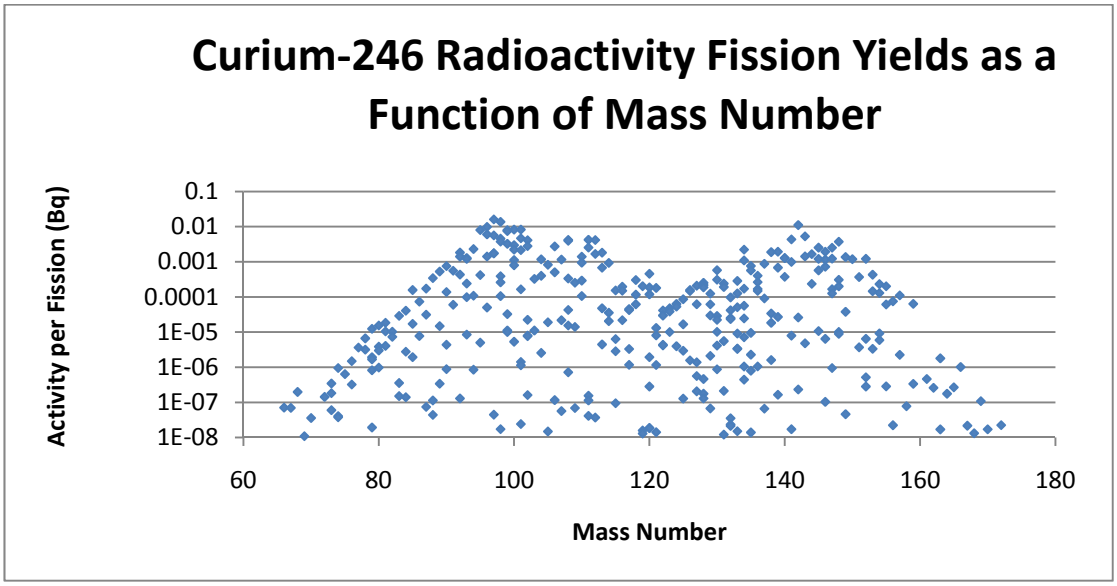

Figure B.8. Curium-246 Radioactivity Yields as a Function of Mass Number.

Appendix C: Activity Estimates of Selected Radionuclides

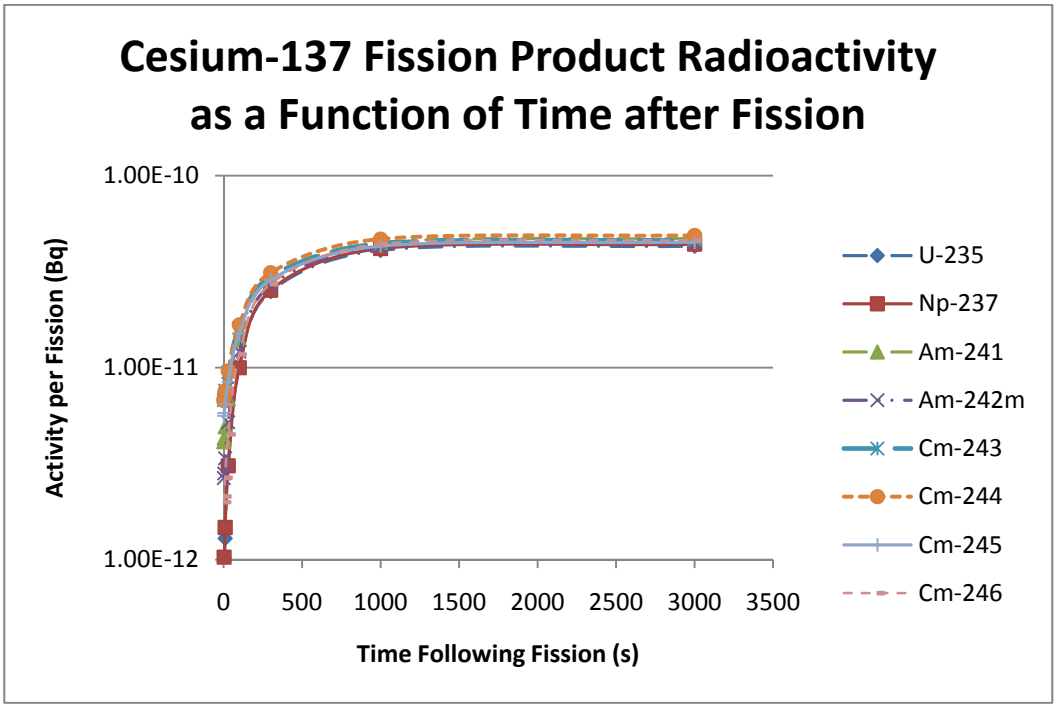

Figure C.1. Cesium-137 Fission Product Radioactivity as a Function of Time after Fission. Based upon the ENDF fission product yields and RSAC calculated radionuclide decay, the activity of ^{137}Cs is relatively independent of the nuclide undergoing fission. This could have significant implications for some technological aspects of MAs; and specifically, the geologic storage of fission product wastes (Forsberg, 2000).

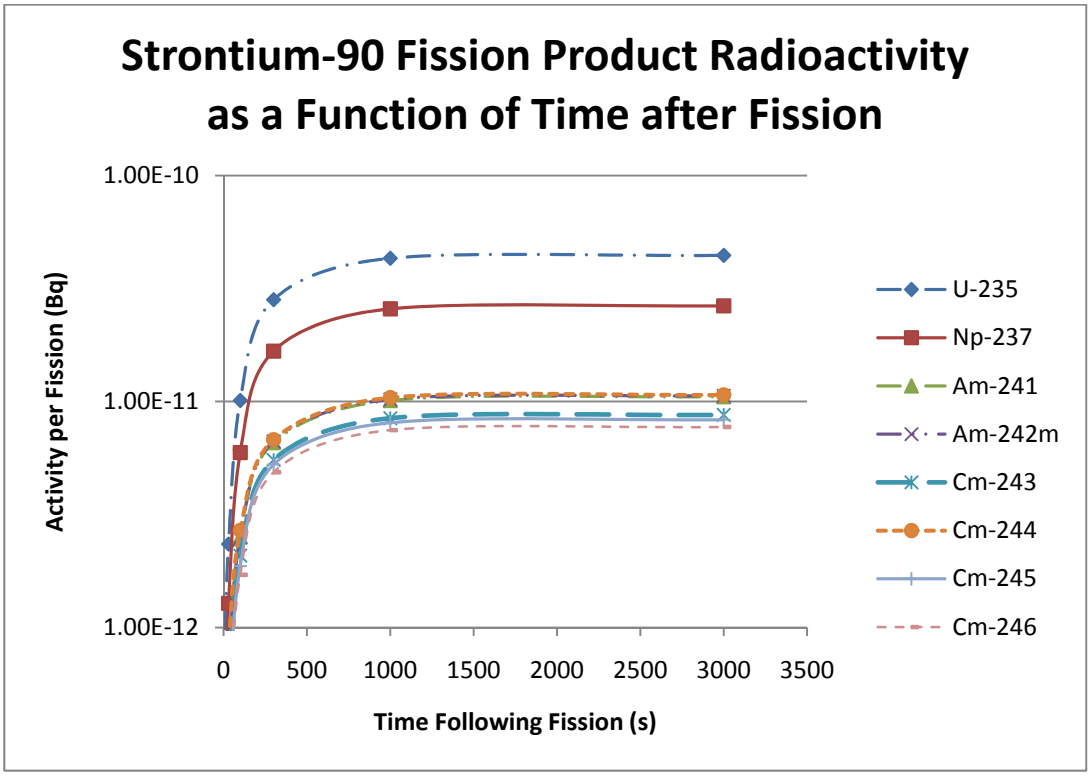

Figure C.2. Strontium-90 Fission Product Radioactivity as a Function of Time after Fission. The analysis of ENDF radionuclide yields in conjunction with the RSAC radiological decay function shows that the ^{90}Sr radioactivity of FP from ^{235}U bounds the ^{90}Sr radioactivity from FP of the other nuclides in this study.

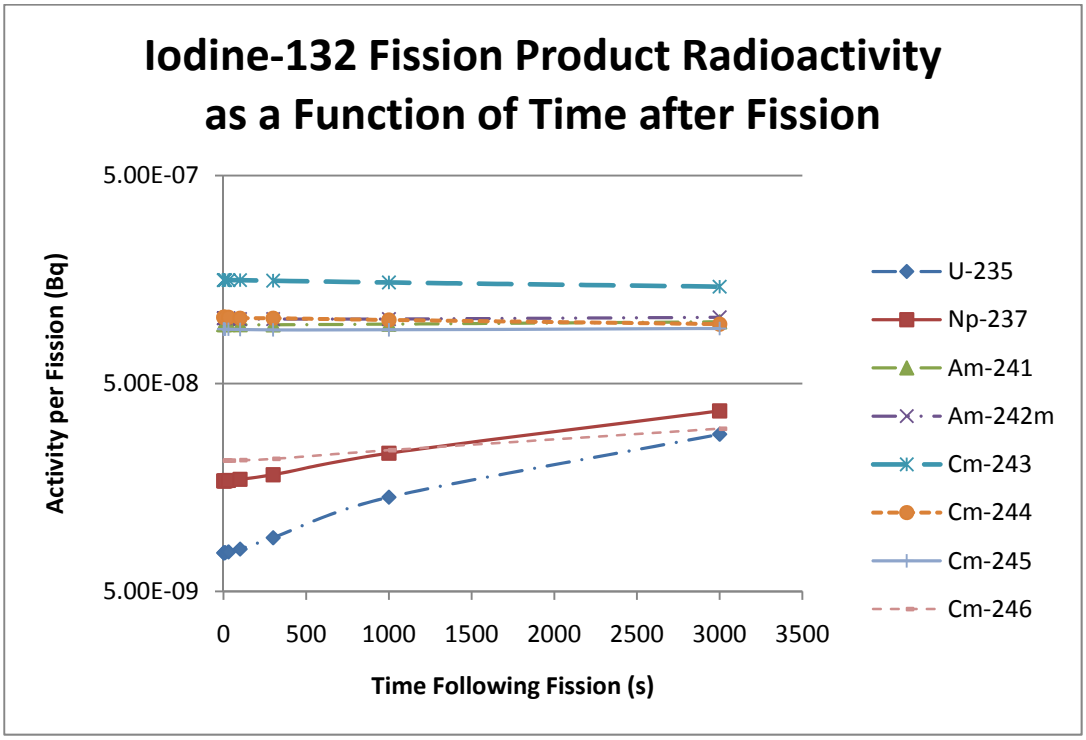

Figure C.3. Iodine-132 Fission Product Radioactivity as a Function of Time after Fission. The ^{132}I radioactivity included in ^{243}Cm FP is estimated to be larger than the ^{132}I content of FP from the other nuclides being evaluated. Note the increase in ^{132}I content, specifically for ^{235}U, ^{237}Np, and ^{246}Cm. This is attributed to the in-growth of ^{132}I resulting from the decay of parent radionuclides.

Appendix D: Determination of Mass Energy Absorption Coefficients and Exposure Rates

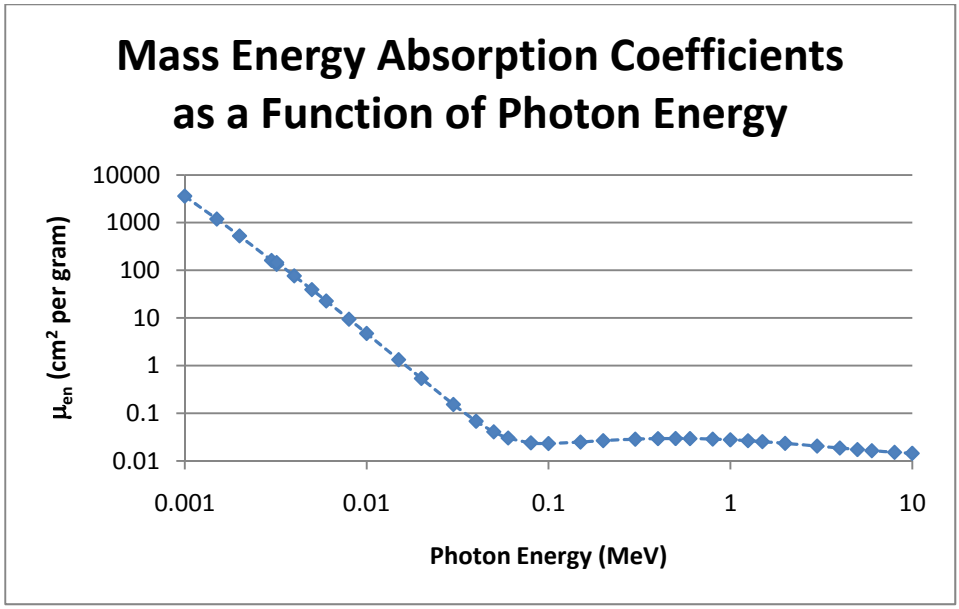

Figure D.1. Mass Energy Absorption Coefficients as a Function of Photon Energy. The data for μ_{en} is shown (Shultis, 2000). Note the significant increase in μ_{en} below photon energies of 0.1 MeV.

Table D.1. Interpolation Expressions for Determining Mass energy absorption coefficients as a Function of Photon Energy. The following expressions were used to computationally determine the mass energy absorption coefficient for each photon emission in the NuDat data that was relevant to the fission product distributions being analyzed. The R^2 values are provided to illustrate the statistical accuracy of each portion of the piecewise function.

Minimum Energy (MeV)	Maximum Energy (MeV)	$\frac{\mu_{en}}{\rho}$ Expression as a Function of Photon Energy, in MeV	R^2 Value
0.001	0.0032	$1E\text{-}05x^{-2.841}$	0.9998
0.0032	0.05	$4E\text{-}06x^{-3.031}$	0.9996
0.05	0.1	$-355.33x^3 + 92.18x^2 - 7.9633x + 0.2531$	1
0.1	0.6	$0.0662x^3 - 0.1152x^2 + 0.0649x + 0.0178$	0.9989
0.6	15	$-6E\text{-}09x^5 + 2E\text{-}06x^4 - 7E\text{-}05x^3 + 0.001x^2 - 0.0066x + 0.0334$	0.9996

This information can also expressed as a function:

$$\frac{\mu_{en}}{\rho}(E) = \begin{cases} 0.00001\mathrm{E}^{-2.841}; & 0.001 < E < 0.0032 \\ 0.000004\mathrm{E}^{-3.031}; & 0.0032 < E < 0.05 \\ -355.33\mathrm{E}^3 + 92.18\mathrm{E}^2 - 7.9633\mathrm{E} + 0.2531; & 0.05 < E < 0.1 \\ 0.0662\mathrm{E}^3 - 0.1152\mathrm{E}^2 + 0.0649\mathrm{E} + 0.0178; & 0.1 < E < 0.6 \\ -6 \cdot 10^{-9}\mathrm{E}^5 + 2 \cdot 10^{-6}\mathrm{E}^4 - 7 \cdot 10^{-5}\mathrm{E}^3 + 0.001\mathrm{E}^2 - 0.0066\mathrm{E} + 0.0334; & 0.6 < E < 15 \end{cases}$$

Table D.2. Comparison of Calculated Exposure Rate Values with Published Exposure Rate Data. As acceptability criteria, the results of calculations for selected nuclides of interest were compared with publicized data for the exposure rate constants of these nuclides. As shown below, somewhat reasonable agreement was demonstrated.

Nuclide	Calculated Specific Gamma Ray Constant ($R\ m^2$ per Ci h)	Published Specific Gamma Ray Constant ($R\ m^2$ per Ci h)	Difference (%)
Cs-137	0.370	0.382	-3.14
I-131	0.266	0.283	-6.00

Appendix E: Risk Estimates

Table E.1. Ordered Risks (by Nuclide) Immediately after Fission. For age groups 0-5 years and 0-110 years, the estimated risks posed by the FP of each nuclide were ordered. Using available data, there were three nuclides whose FP produced risks that were estimated to be greater than those of ^{235}U.

Inhalation	Ingestion	External (Submersion)
Am-241	Am-241	Am-241
Cm-244	Cm-244	Cm-244
Cm-243	Cm-243	Cm-243
U-235	U-235	U-235
Am-242m	Am-242m	Am-242m
Np-237	Np-237	Np-237
Cm-245	Cm-245	Cm-245
Cm-246	Cm-246	Cm-246

Table E.2. Ordered Inhalation Risks (by location) Immediately after Fission (0-5 years). Using available data, the colon thyroid, and lung were the sites subjected to the greatest risk from inhalation of FP in the 0 to 5 year age group.

U-235	Np-237	Am-241	Am-242m	Cm-243	Cm-244	Cm-245	Cm-246
Total	Total	Total	Total	Total	Total	Total	Total
Colon	Thyroid	Colon	Thyroid	Colon	Colon	Thyroid	Thyroid
Thyroid	Colon	Lung	Colon	Lung	Lung	Colon	Colon
Lung	Lung	Thyroid	Lung	Thyroid	Thyroid	Lung	Lung
Stomach	Stomach	Stomach	Stomach	Stomach	Stomach	Stomach	Stomach
Residual	Residual	Residual	Residual	Residual	Residual	Residual	Residual
Breast	Breast	Breast	Breast	Breast	Breast	Breast	Breast
Leukemia	Bladder	Leukemia	Leukemia	Leukemia	Leukemia	Bladder	Leukemia
Bladder	Leukemia	Bladder	Bladder	Bladder	Bladder	Leukemia	Bladder
Ovary	Ovary	Ovary	Ovary	Ovary	Ovary	Ovary	Ovary
Esophagus	Esophagus	Esophagus	Esophagus	Esophagus	Esophagus	Esophagus	Esophagus
Liver	Liver	Liver	Liver	Liver	Liver	Liver	Liver
Kidney	Kidney	Kidney	Kidney	Kidney	Kidney	Kidney	Kidney
Bone	Bone	Bone	Bone	Bone	Bone	Bone	Bone
Skin	Skin	Skin	Skin	Skin	Skin	Skin	Skin

Table E.3. Ordered Inhalation Risks (by location) Immediately after Fission (0-110 years). Similar to Table E.2, the risks for the 0-110 year age group show that the thyroid and colon are secondary considerations to the risks posed to the lungs.

U-235	Np-237	Am-241	Am-242m	Cm-243	Cm-244	Cm-245	Cm-246
Total	Total	Total	Total	Total	Total	Total	Total
Lung	Lung	Lung	Lung	Lung	Lung	Lung	Lung
Colon	Thyroid	Colon	Thyroid	Colon	Colon	Thyroid	Thyroid
Thyroid	Colon	Stomach	Colon	Thyroid	Stomach	Colon	Colon
Stomach	Stomach	Thyroid	Stomach	Stomach	Thyroid	Stomach	Stomach
Residual	Residual	Residual	Residual	Residual	Residual	Residual	Residual
Bladder	Bladder	Breast	Bladder	Bladder	Breast	Bladder	Bladder
Breast	Breast	Bladder	Breast	Breast	Leukemia	Breast	Breast
Leukemia	Leukemia	Leukemia	Leukemia	Leukemia	Bladder	Leukemia	Leukemia
Ovary	Ovary	Ovary	Ovary	Ovary	Ovary	Ovary	Ovary
Liver	Liver	Liver	Liver	Liver	Liver	Liver	Liver
Esophagus	Esophagus	Esophagus	Esophagus	Esophagus	Esophagus	Esophagus	Esophagus
Kidney	Kidney	Kidney	Kidney	Kidney	Kidney	Kidney	Kidney
Bone	Bone	Bone	Bone	Bone	Bone	Bone	Bone
Skin	Skin	Skin	Skin	Skin	Skin	Skin	Skin

Table E.4. Ordered Ingestion Risks (by location) Immediately after Fission. The risks posed by ingestion differ slightly from the inhalation risks shown above. The colon is the site subject to the greatest risk based upon available data.

U-235	Np-237	Am-241	Am-242m	Cm-243	Cm-244	Cm-245	Cm-246
Total	Total	Total	Total	Total	Total	Total	Total
Colon	Colon	Colon	Colon	Colon	Colon	Colon	Colon
Stomach	Stomach	Stomach	Stomach	Stomach	Stomach	Thyroid	Stomach
Thyroid	Thyroid	Thyroid	Thyroid	Thyroid	Thyroid	Stomach	Thyroid
Residual	Residual	Residual	Residual	Residual	Residual	Residual	Residual
Lung	Lung	Lung	Lung	Lung	Lung	Lung	Lung
Breast	Breast	Breast	Breast	Breast	Breast	Breast	Breast
Ovary	Bladder	Ovary	Ovary	Ovary	Ovary	Bladder	Bladder
Bladder	Ovary	Bladder	Bladder	Bladder	Bladder	Ovary	Ovary
Leukemia	Leukemia	Leukemia	Leukemia	Leukemia	Leukemia	Leukemia	Leukemia
Liver	Liver	Liver	Liver	Liver	Liver	Liver	Liver
Kidney	Kidney	Kidney	Kidney	Kidney	Kidney	Kidney	Kidney
Esophagus	Esophagus	Esophagus	Esophagus	Esophagus	Esophagus	Esophagus	Esophagus
Bone	Bone	Bone	Bone	Bone	Bone	Bone	Bone
Skin	Skin	Skin	Skin	Skin	Skin	Skin	Skin

The information contained in Figures E.1 through E.8 are directly affected by the risk factor data (or lack thereof) published in FGR 13. An important consideration noted in FGR 13 is that many nuclides with half-lives less than 10 minutes were not included in risk factor development. As a result, many short-lived fission product radionuclides lack risk factor data. This is reflected in the general behavior noted in Figures E.1 through E.8. The increases in risk observed in the figures are most likely not due to a true increase in risk, but due to the decay of a short-lived radionuclide without risk factor data into a longer-lived radionuclide with published risk factor data. As a result, the uncertainties on risk factor estimates, and specifically those below 10 minutes, should be viewed as uncertain at best.

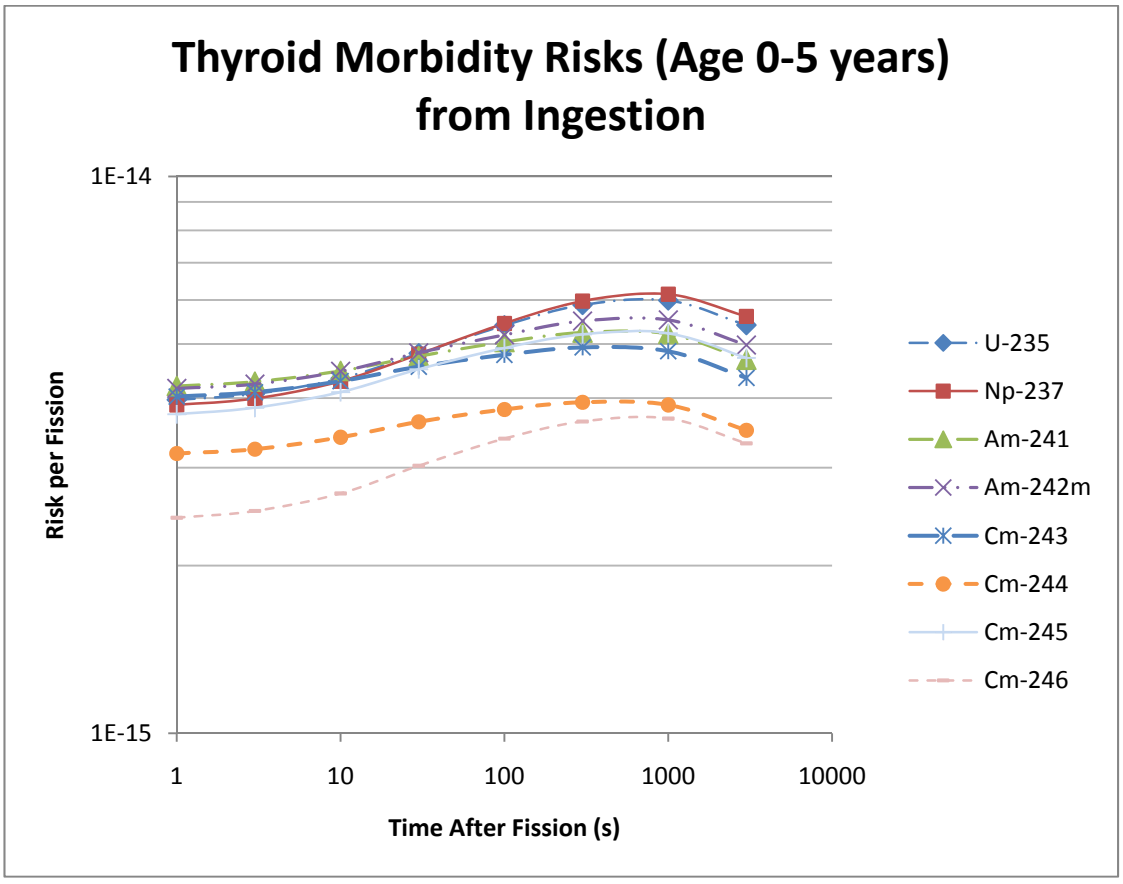

Figure E.1. Thyroid Morbidity Risks (Age 0-5 years) from Ingestion.

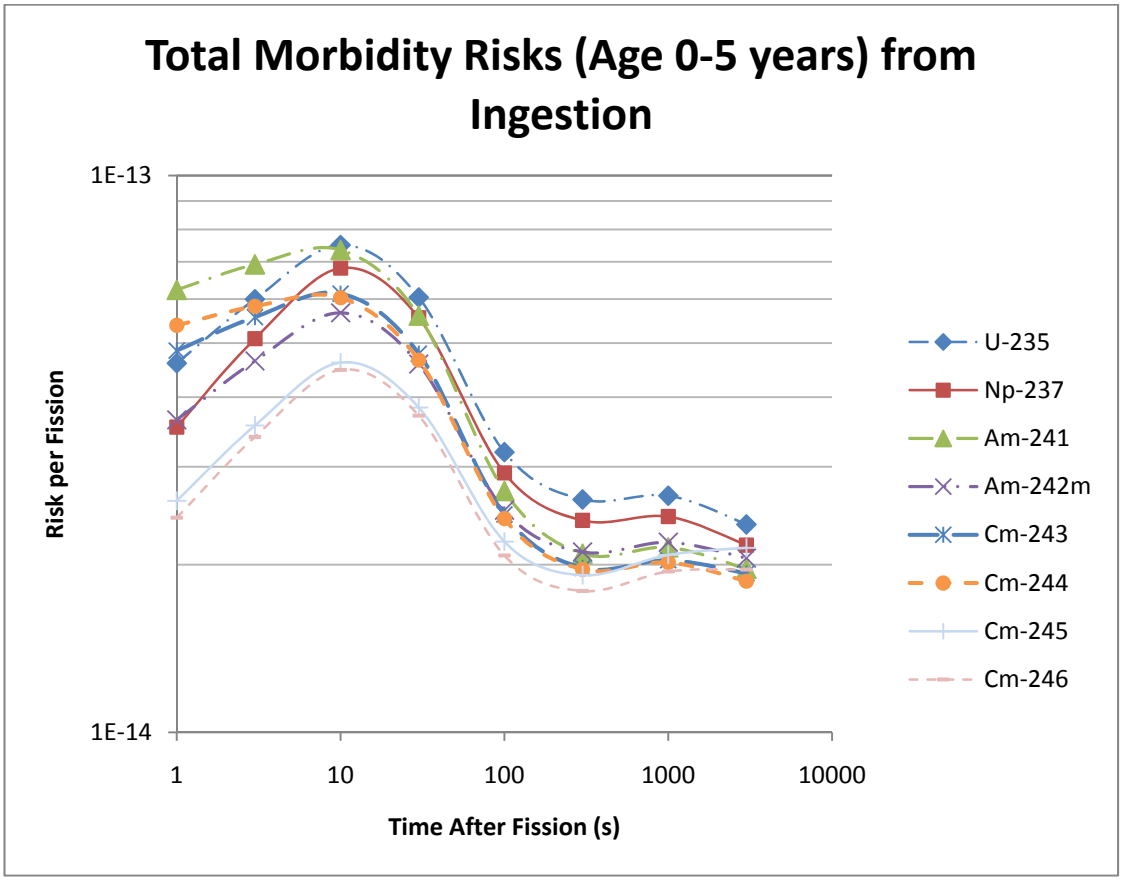

Figure E.2. Total Morbidity Risks (Age 0-5 years) from Ingestion.

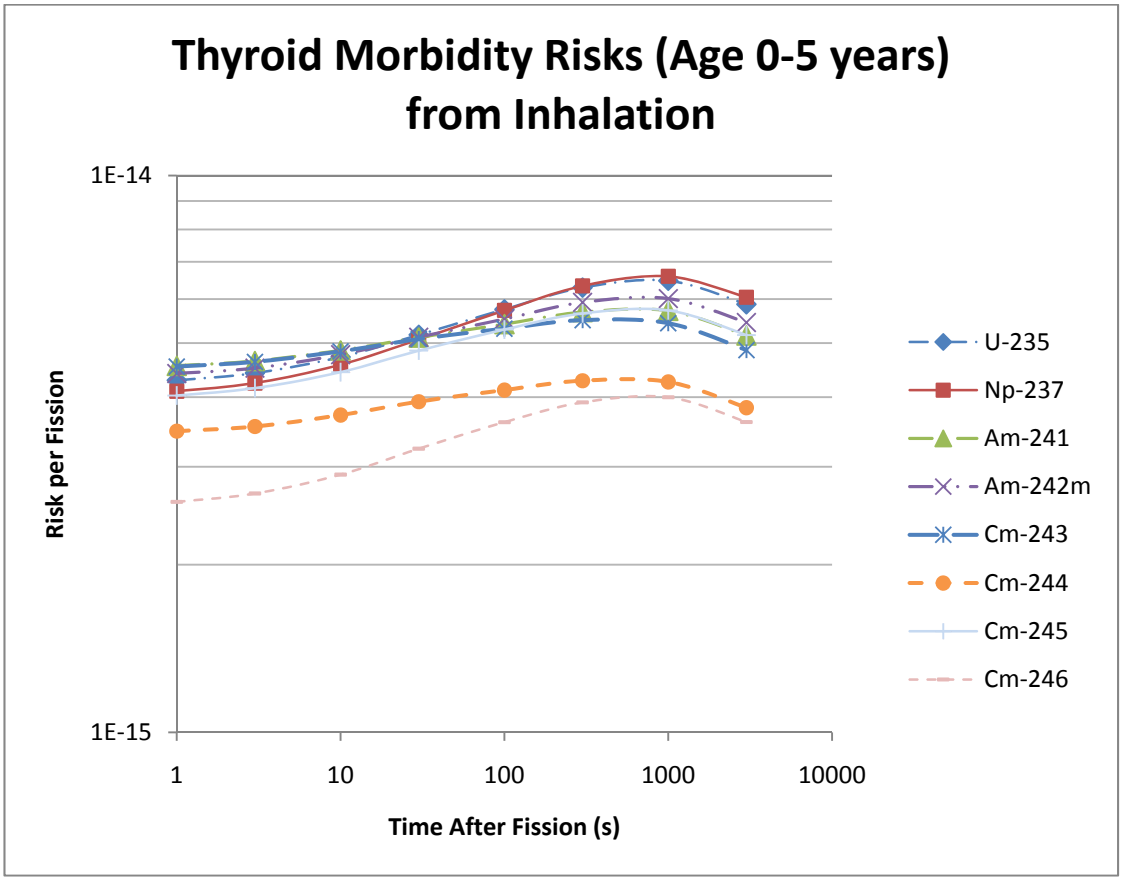

Figure E.3. Thyroid Morbidity Risks (Age 0-5 years) from Inhalation.

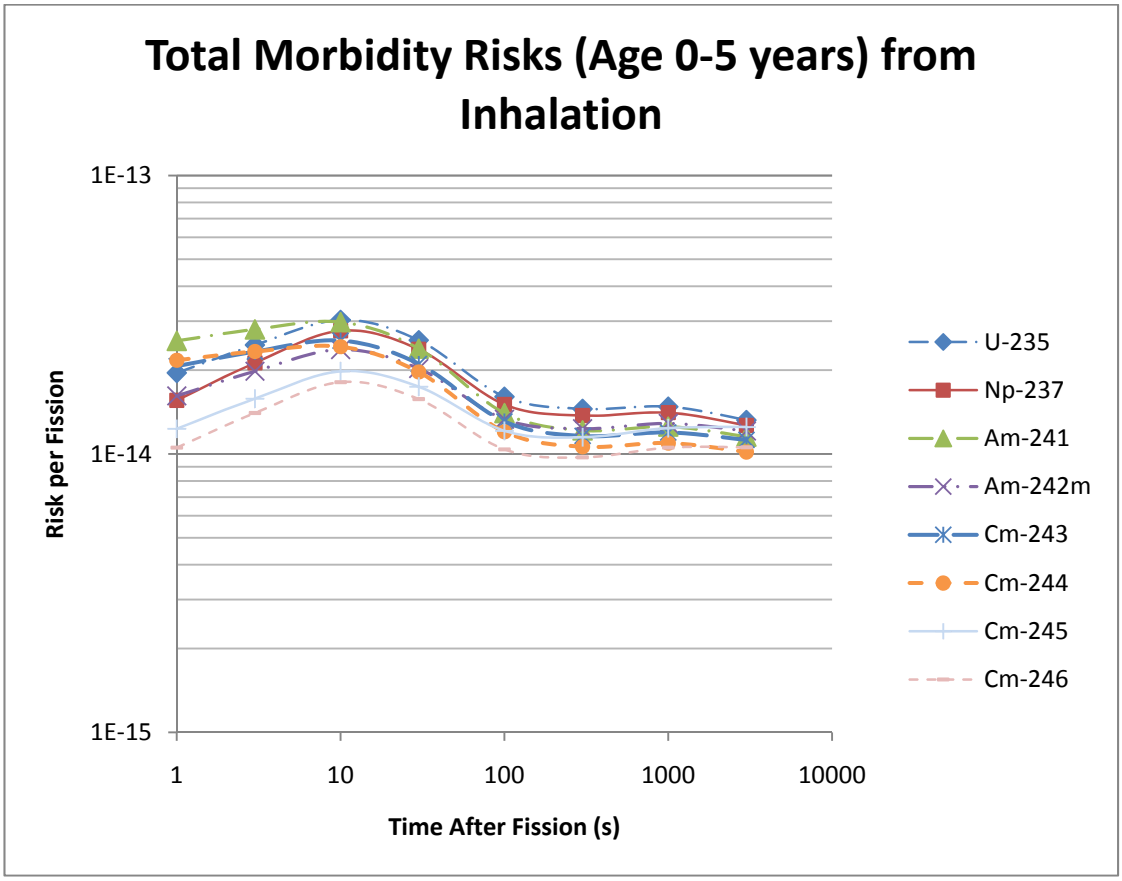

Figure E.4. Total Morbidity Risks (Age 0-5 years) from Inhalation.

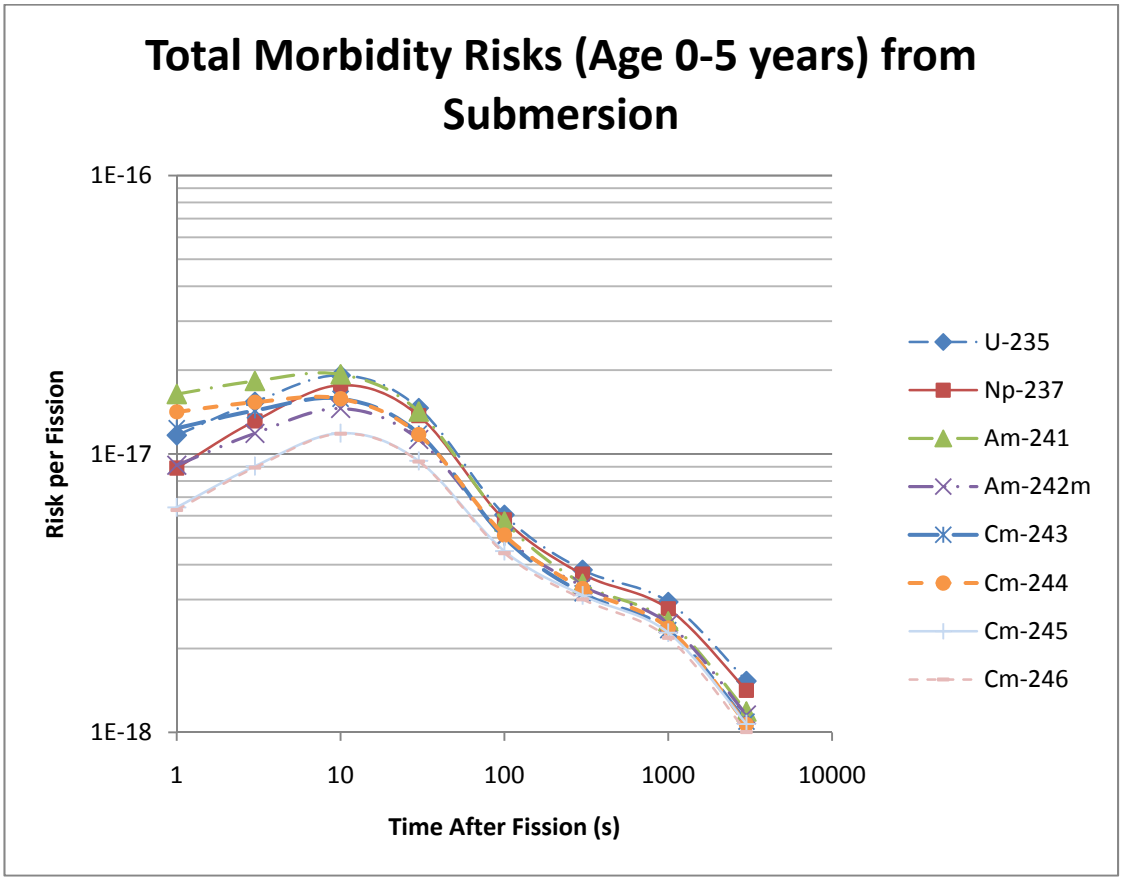

Figure E.5. Total Morbidity Risks (Age 0-5 years) from Submersion.

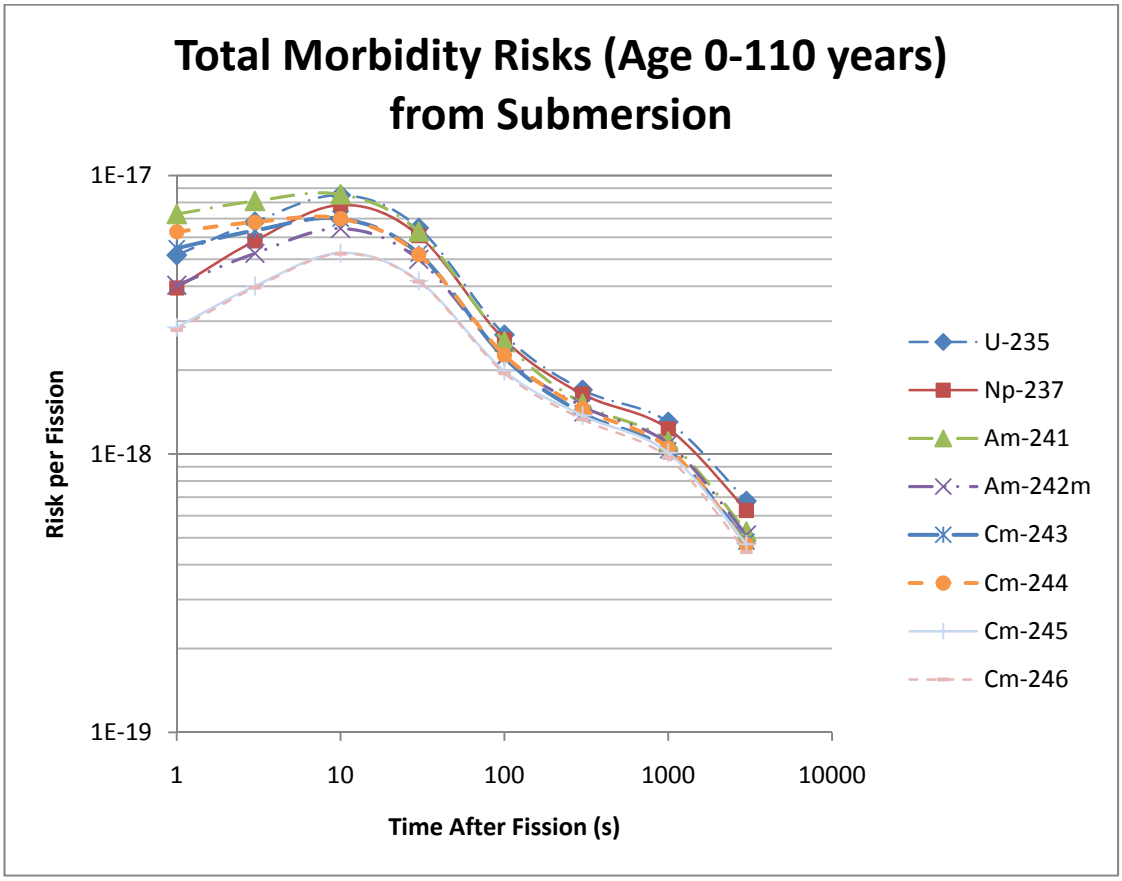

Figure E.6. Total Morbidity Risks (Age 0-110 years) from Submersion.

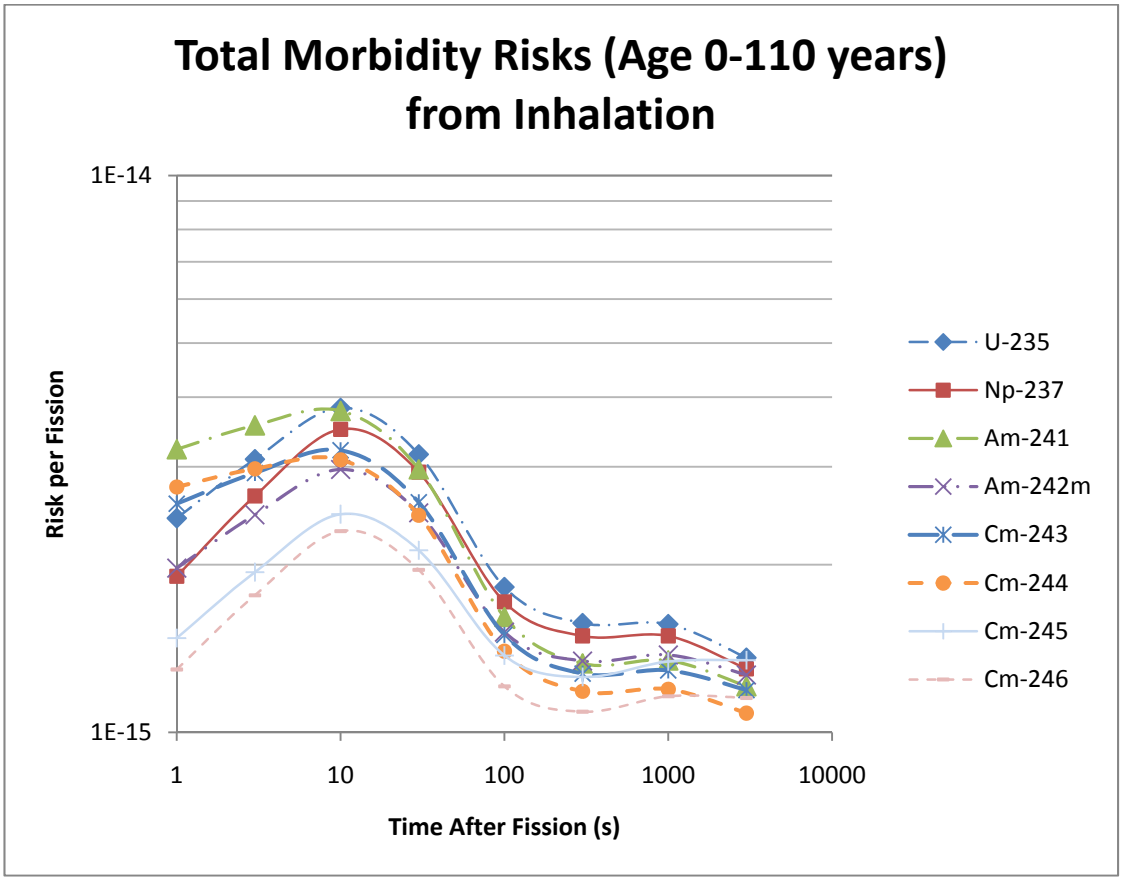

Figure E.7. Total Morbidity Risks (Age 0-110 years) from Inhalation.

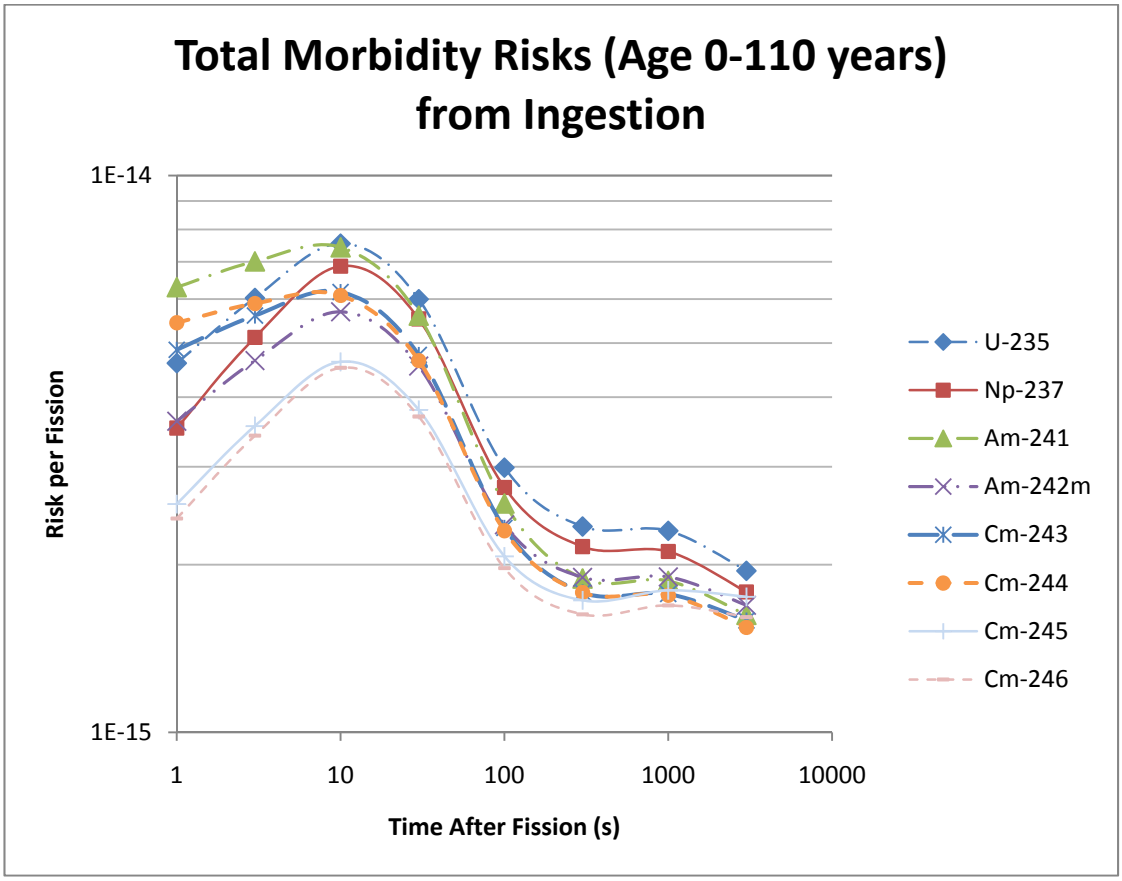

Figure E.8. Total Morbidity Risks (Age 0-110 years) from Ingestion.

Appendix F: RSAC Analyses

Table F.1. Radionuclides Neglected from RSAC Analyses. The following nuclides were absent from RSAC radiological libraries and the ICRP-30 dose conversion factor database. Many of these nuclides have short half-lives.

Ag-105	Dy-167	I-121	Ni-67	Sn-130m1
Ag-105m1	Dy-168	I-132m1	Ni-69	Sr-83
Ag-107m1	Dy-169	In-109	Ni-70	Sr-87
Ag-115m1	Er-163	In-112m1	Pd-116	Sr-96
Ag-116	Er-165	In-112m2	Pr-139	Tb-155
Ag-116m1	Er-167m1	In-116	Pr-140	Tb-156
Ag-117m1	Er-172	In-119	Pr-148m1	Tb-156m1
Ag-120m1	Eu-149	In-122	Pr-150	Tb-158m1
Ag-122	Eu-154m1	In-122m1	Rb-101	Tb-162
As-82	Ga-74m1	In-124m1	Rb-86m1	Tb-163
As-82m1	Gd-151	In-126m1	Rb-96	Tb-164
Ba-136m1	Gd-161	In-128m1	Rh-104	Tb-165
Br-77m1	Gd-162	In-129m1	Rh-104m1	Tb-166
Br-78	Gd-163	In-130m1	Rh-110	Tc-100
Br-79m1	Ge-71m1	In-131m1	Rh-110m1	Tc-95
Cd-107	Ge-73m1	Kr-79m1	Rh-116	Tc-95m1
Cd-121m1	Ge-78m1	Kr-81m1	Rh-117	Tm-165
Cd-122	Ge-79m1	La-135	Ru-107	Tm-166
Ce-137	Ho-159	La-146m1	Ru-110	Tm-167
Ce-139m1	Ho-159m1	Lu-171	Sb-118	Tm-168
Co-66	Ho-161	Lu-171m1	Sb-118m1	Tm-172
Co-67	Ho-162	Lu-172	Sb-119	Y-89m1
Co-68	Ho-162m1	Lu-172m1	Sb-120	Y-93m1
Cu-66	Ho-163m1	Mo-110	Sb-120m1	Y-96
Cu-68	Ho-167	Nb-90	Sb-122m1	Y-96m1
Cu-68m1	Ho-168	Nb-91	Sb-124m1	Y-97m1
Cu-69	Ho-169	Nb-91	Sb-124m2	Y-98m1
Cu-70	Ho-170	Nb-92	Se-77m1	Yb-169m1
Cu-70m1	Ho-170m1	Nb-92	Sn-113m1	Zn-71
Dy-165m1	Ho-172	Ni-66	Sn-128m1	Zr-90m1

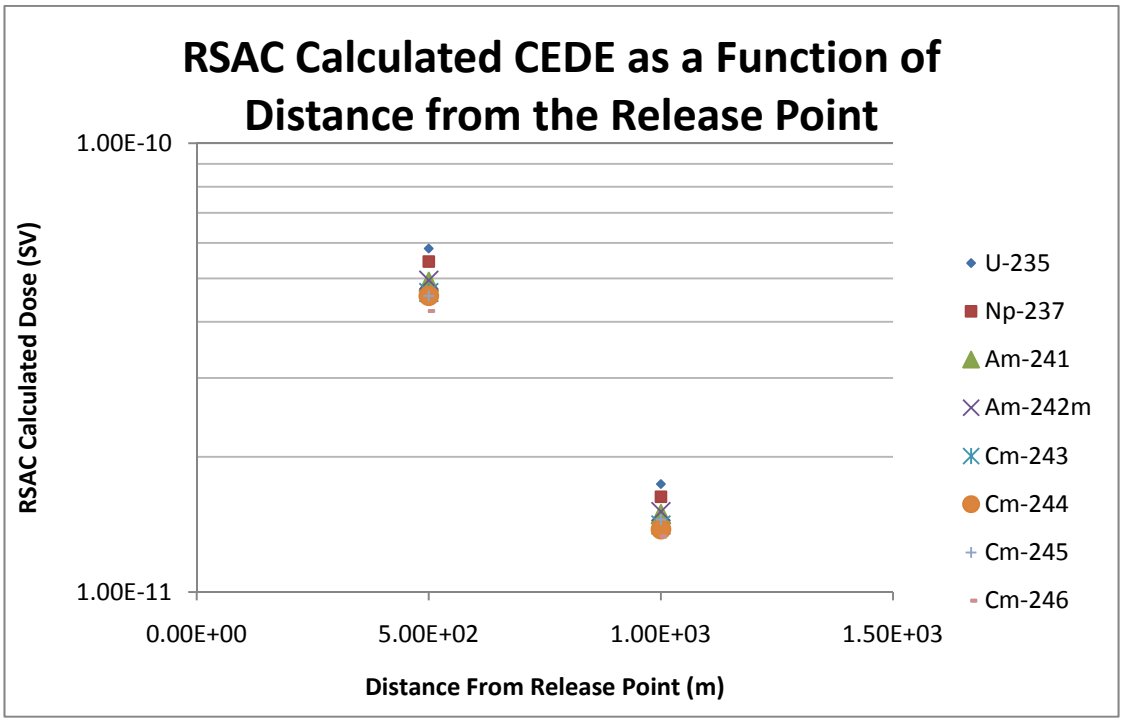

Figure F.1. RSAC Calculated CEDEs as a Function of Distance from the Release Point (Detail). A detailed view of the RSAC results for CEDEs between 0 and 1500 meters shows that ^{235}U and ^{237}Np produce the greatest estimated CEDEs for the simulated release.

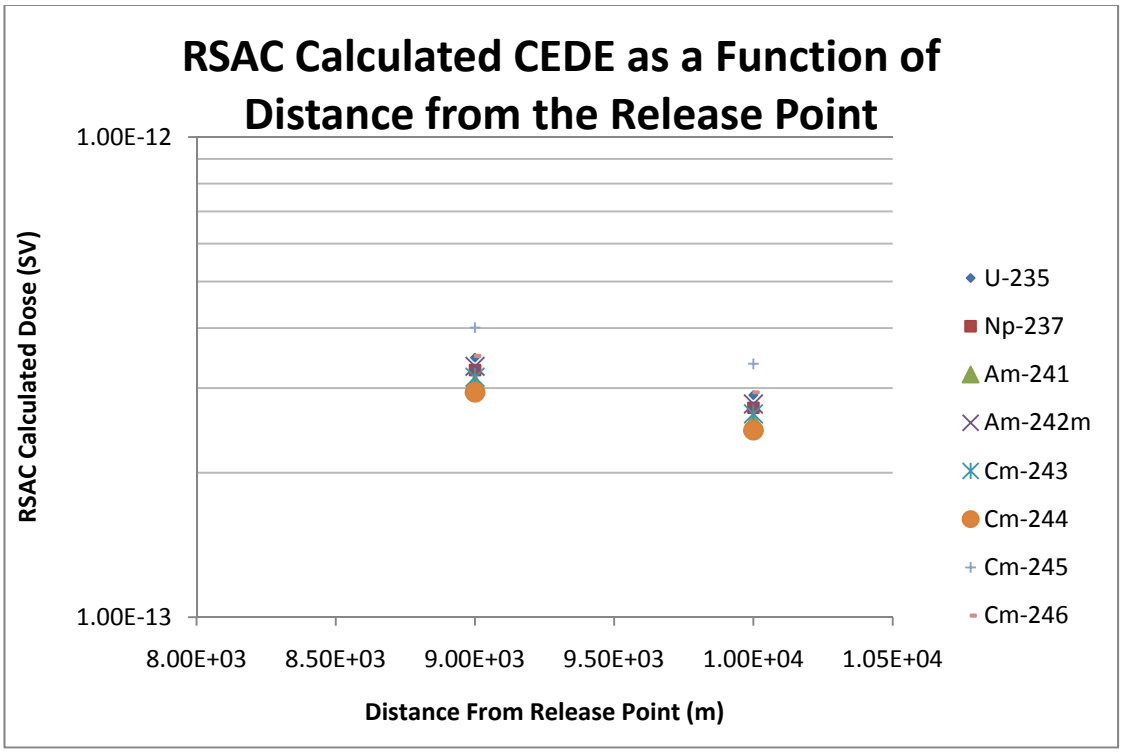

Figure F.2. RSAC Calculated CEDEs as a Function of Distance from the Release Point (Detail). A detailed view of the RSAC results for CEDEs between 8000 and 10500 meters shows that ^{245}Cm and ^{246}Cm produce the greatest estimated CEDEs for the simulated release.

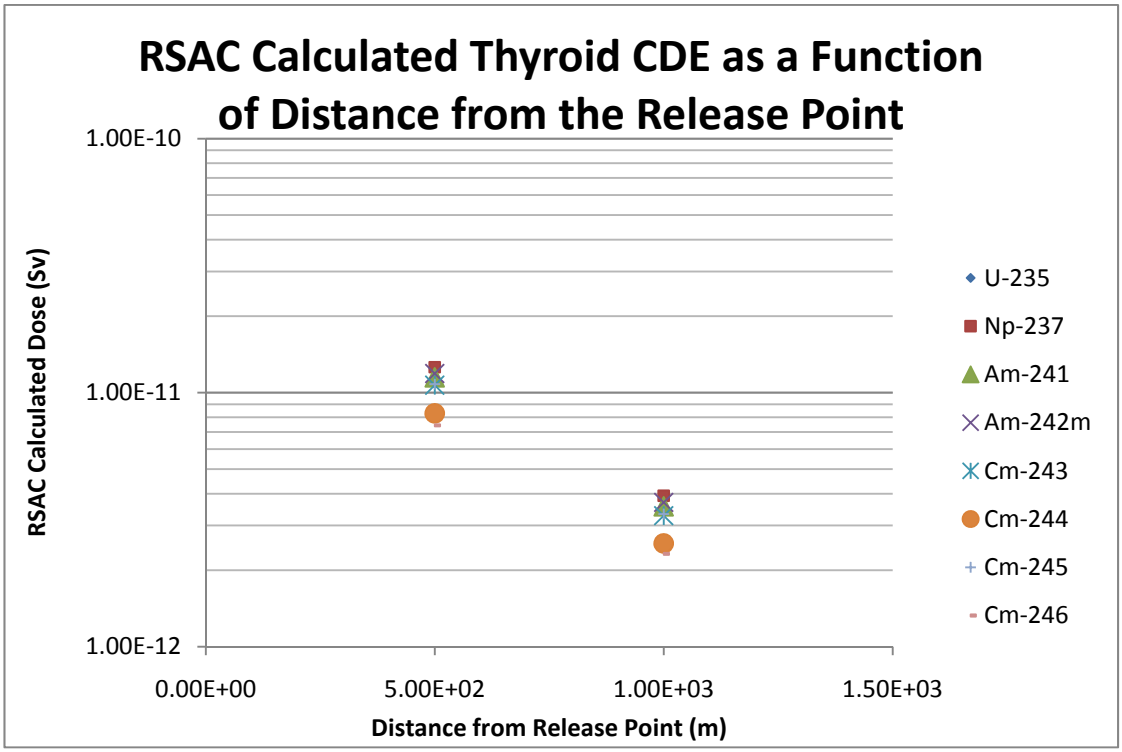

Figure F.3. RSAC Calculated Thyroid CDEs as a Function of Distance from the Release Point (Detail). The RSAC calculations show that, for distances of 0 to 1500 m, ^{237}Np results in the greatest estimated thyroid dose.

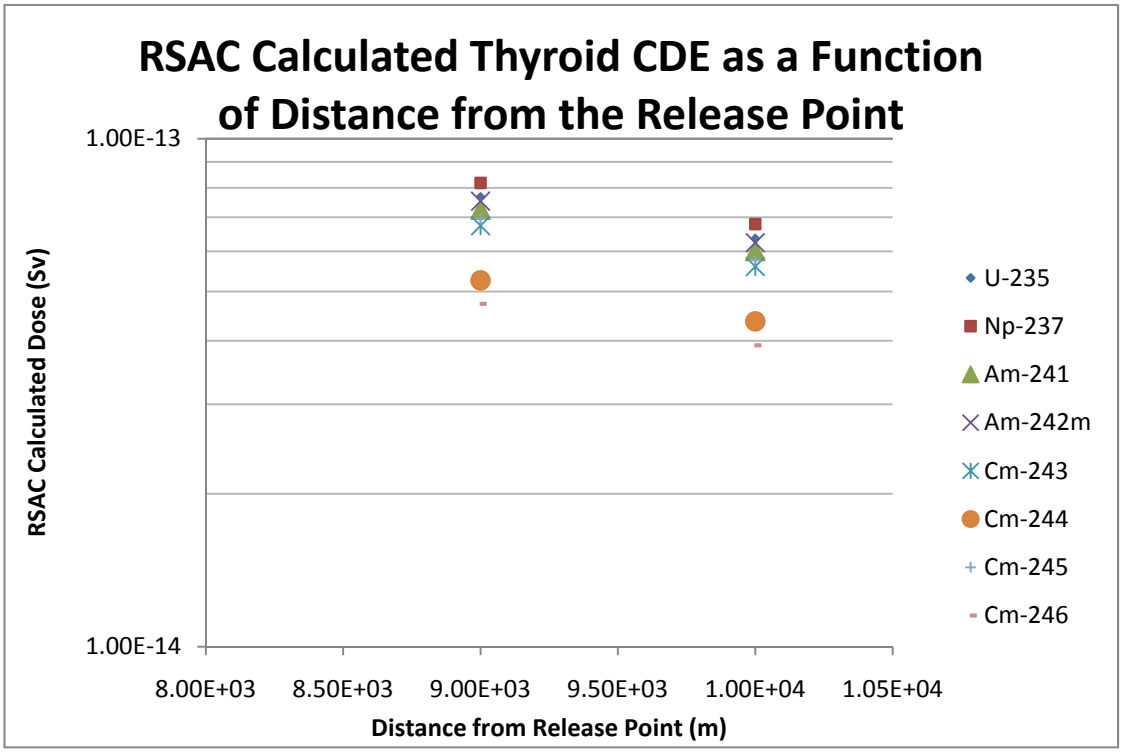

Figure F.4. RSAC Calculated Thyroid CDEs as a Function of Distance from the Release Point (Detail). The RSAC results, when examined from 8000 to 10500 m, show that ^{237}Np again presents the greatest risk to the thyroid, with ^{235}U and the other nuclides posing less of a risk.

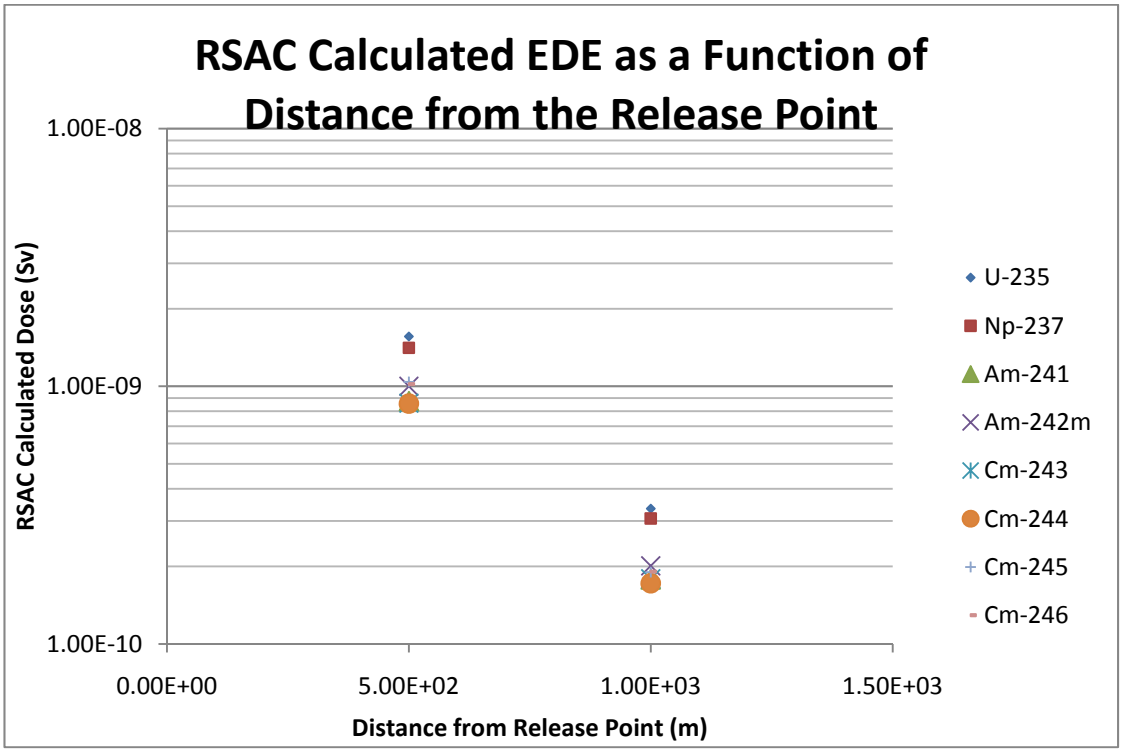

Figure F.5. RSAC Calculated EDEs as a Function of Distance from the Release Point (Detail). The detail of the RSAC results for distances from 0 to 1500 m are shown above, with the EDEs from ^{237}Np and ^{235}U FP estimated to be larger than the EDEs of the other FP.

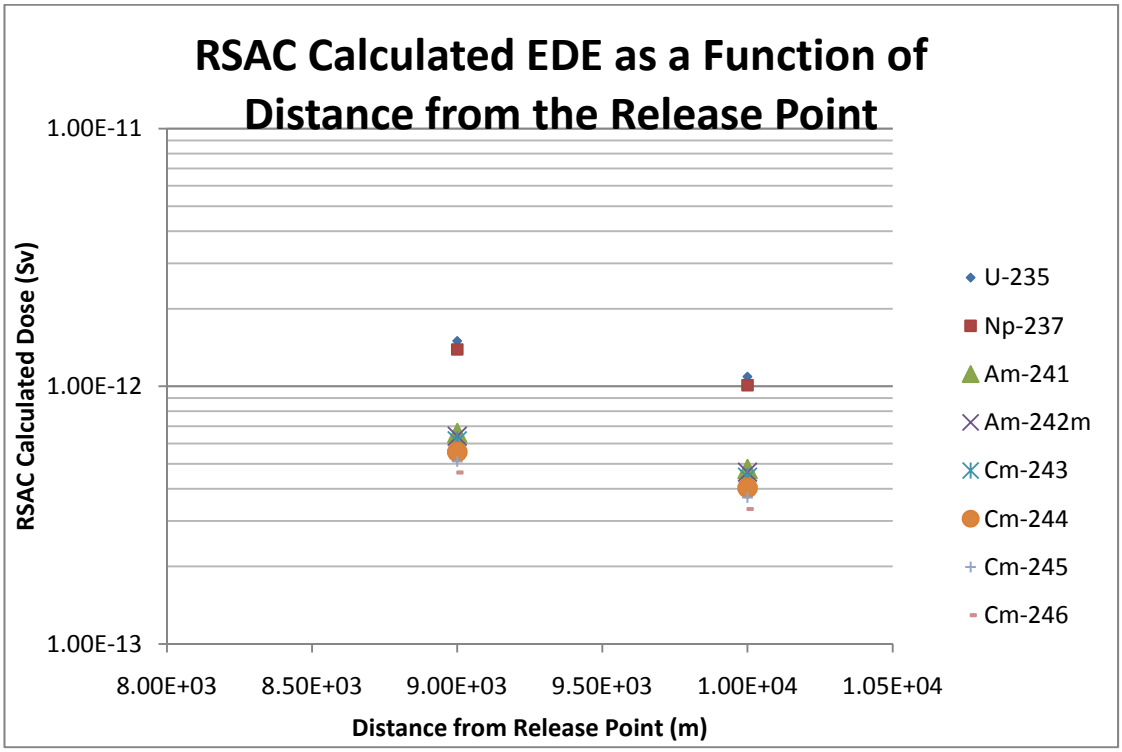

Figure F.6. RSAC Calculated EDEs as a Function of Distance from the Release Point (Detail). The detail of the RSAC results for distances from 8000 to 10500 m are shown above, with the EDEs from ^{237}Np and ^{235}U FP estimated to be larger than the EDEs of the other FP.

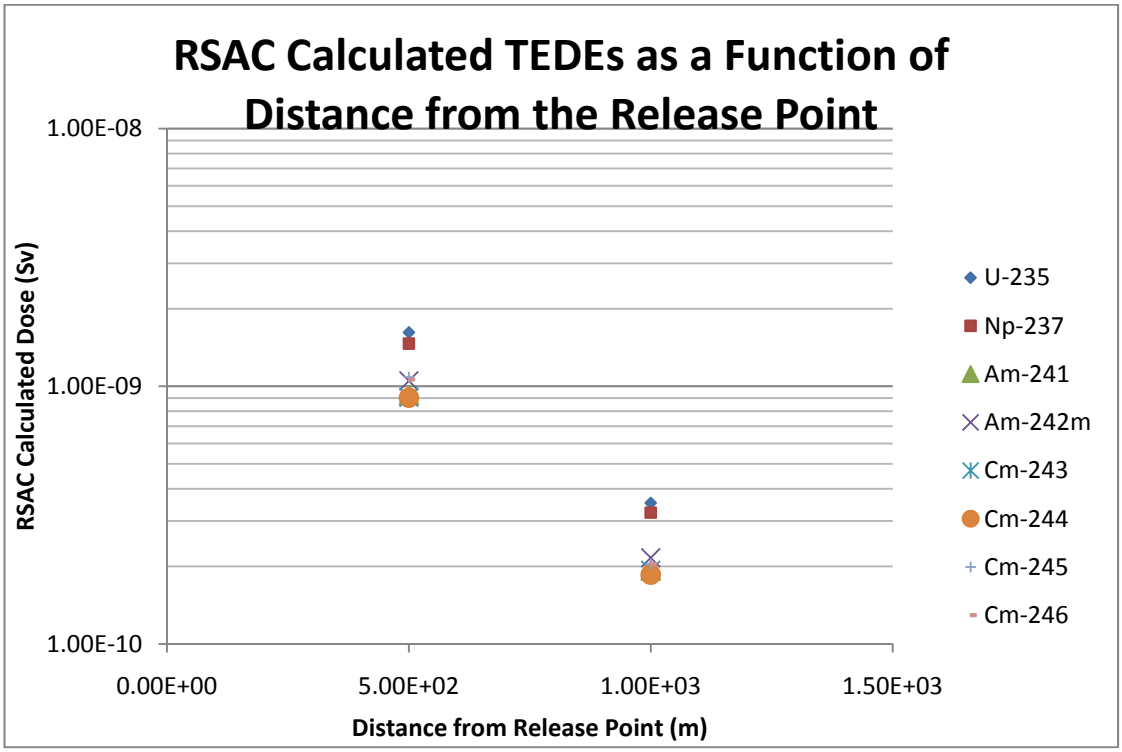

Figure F.7. RSAC Calculated TEDEs as a Function of Distance from the Release Point (Detail). A detail of the TEDE results for 0 to 1500 m show that doses from ^{235}U and ^{237}Np are estimated to be the largest.

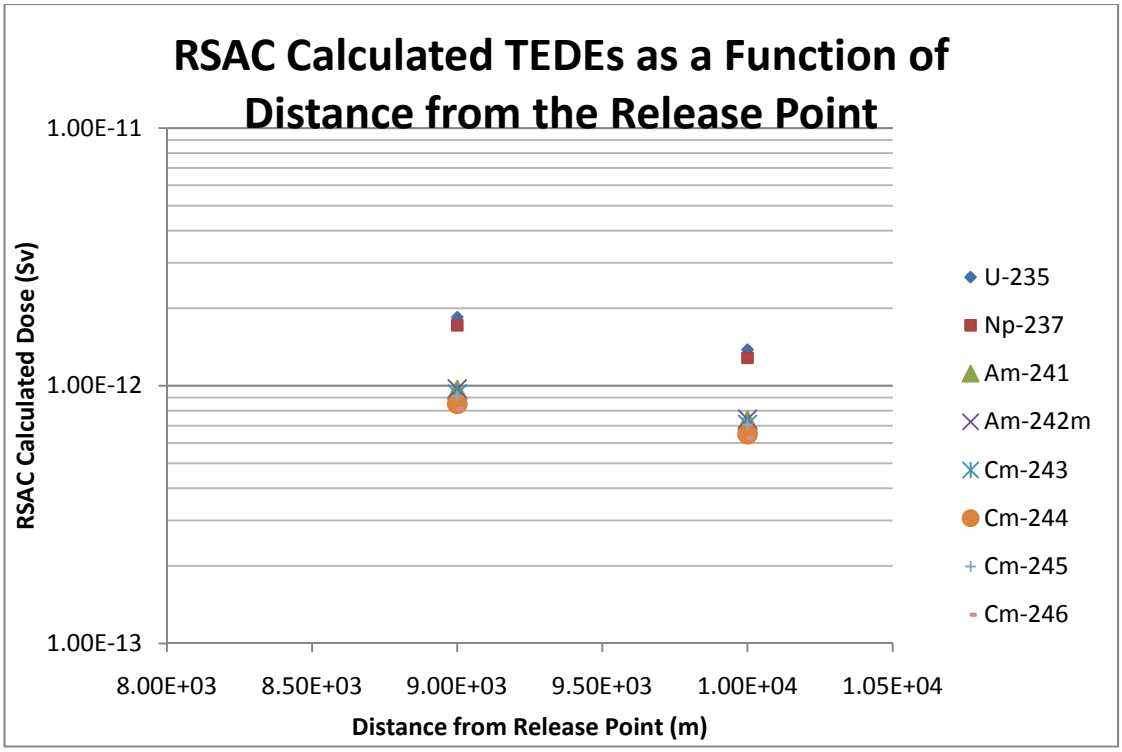

Figure F.8. RSAC Calculated TEDEs as a Function of Distance from the Release Point (Detail). The RSAC calculated TEDEs for instantaneous fission product releases at distances of 8000 to 10500 m. Results are similar to the EDE results at these distances.